C.P. No. 1057

MINISTRY OF TECHNOLOGY

AERONAUTICAL RESEARCH COUNCIL

CURRENT PAPERS

Performance Estimates for a Reflected-Shock Tunnel with a Modified Driver to produce High Test-Section Reynolds Numbers

by

J. G. Woodley

Aerodynamics Dept., R.A.E., Farnborough

LONDON. HER MAJESTY'S STATIONERY OFFICE

1969

NINE SHILLINGS NET

U.D.C. 533.6.071.8 : 533.6.071.4

C.P. No.1057*
November 1968

PERFORMANCE ESTIMATES FOR A REFLECTED-SHOCK TUNNEL WITH A MODIFIED DRIVER TO PRODUCE HIGH TEST-SECTION REYNOLDS NUMBERS

by

J. G. Woodley
Aerodynamics Dept., R.A.E., Farnborough

SUMMARY

Some calculations based on the performance of an ideal shock-tube are presented. These demonstrate the possibility of achieving a high test-section Reynolds number in a reflected-shock tunnel, employing nitrogen or air as the test gas, by the use of a driver gas composed of a mixture of hydrogen and nitrogen.

* Replaces R.A.E. Technical Report 68272 - A.R.C. 31263

CONTENTS

1 INTRODUCTION

The R.A.E. 15" reflected-shock tunnel was developed originally to provide a test facility with the high flow Mach number and total enthalpy needed for re-entry studies employing air or nitrogen as the working fluid. In some recent work[1] sufficient temperature levels in the working section have been obtained to enable experiments on controlled supersonic combustion of hydrogen with air to be performed successfully.

For basic aerodynamic studies, however, operation of this facility at high stagnation temperatures produces low Reynolds numbers in the working section. As a result of this, viscous interactions have a large influence on the flow field around models[2]. In addition, flow visualisation by conventional schlieren and shadowgraph techniques is affected by the low level of ambient density, and some fine details of the flow field, for example in a wake region, may be invisible. Also, at high temperatures, real-gas effects influence the flow through the nozzle, and conditions in the working section are difficult to predict theoretically and to measure experimentally.

In this Report, a study is made of a possible method of improving the Reynolds number in a shock-tunnel facility for aerodynamic testing by employing a mixed driver technique. Results are presented of some calculations, which assume ideal shock tube performance, and it is shown that the mixed driver-gas technique lowers the total enthalpy levels in the system significantly. As a result density levels are much higher, Reynolds numbers are increased, and real-gas effects become less important. Studies of natural transition may indeed be possible under these improved Reynolds number conditions.

2 FACILITY PERFORMANCE WITH A MIXED DRIVER GAS

For high total-enthalpy operation of the R.A.E. 15" reflected-shock tunnel a light driver-gas, H_2, is used. Because of the high initial speed of sound in this gas a fast primary shock is produced for a minimum ratio of driver gas (H_2) pressure to test gas (N_2 or air) pressure. In order to optimise the running time, operation of the tunnel at or near a primary-shock Mach number, M_T, is arranged such that 'tailoring' conditions will occur after shock wave reflection from the end wall of the shock tube. (See Fig.1a and section 3.2 later.)

To reduce the total enthalpy of the flow behind the reflected shock wave, lower primary-shock Mach numbers are necessary. However, using H_2 as the driver gas at a reduced initial pressure ratio (p_4/p_1) to achieve this would mean operating in grossly under-tailored conditions with a corresponding reduction in running time. Hence one must employ a driver gas with a lower speed of sound than H_2 such that when one is driving shocks into N_2 (or air) the Mach number for tailoring will also be low. A mixture of hydrogen and nitrogen provides a suitable driver in this case and allows some flexibility in the choice of mixture to produce the required conditions.

3 PERFORMANCE CALCULATIONS FOR A MIXED DRIVER GAS

In all the calculations made, 'ideal' flow in the shock tube has been assumed. Thus viscous effects such as shock wave attenuation have been neglected and perfect diaphragm bursting has been assumed. However, some discussion is given in section 4.3 on the validity of these results when conditions are 'non-ideal'.

Formulae and references required for calculations in this section are quoted in the Appendix, and the notation for the various flow regimes in the reflected-shock tunnel are illustrated in Fig.1. Calculations have been based strictly on N_2 as the test gas, but are assumed in the text to be appropriate to air operation also.

3.1 Properties of an hydrogen/nitrogen gas mixture

Fig.2 show how the speed of sound a_x (= a_4) and mean molecular weight, m_x, vary for a gas mixture of H_2 and N_2 as the particle concentration parameter, x, varies from 0 to 1. This parameter x is defined as the ratio of the number of molecules of H_2 to the number of molecules of mixture in a unit volume. Hence x = 0 corresponds to the case of pure N_2, and x = 1 represents the case of pure H_2.

Fig.3 gives the particle concentration parameter in terms of the initial pressure of N_2, p_1, which is increased by addition of H_2 in order to obtain a particular final pressure of the driver gas mixture, p_f (= p_4).

3.2 Reservoir conditions in the test gas

A diagram showing possible modes of operation of a reflected-shock tunnel is given in Fig.1a, b and c. The tailored case Fig.1a was referred to earlier. This is the condition whereby the contact surface behind the primary

shock wave is brought to rest upon interaction with the reflected shock wave, and as a result the maximum flow duration with constant stagnation conditions is obtained in the tunnel working section. The primary shock Mach number, M_s, giving the tailoring condition as a function of the particle concentration x in the mixed driver gas is denoted by M_T in Fig.4.

Fig.5 shows, for a given value of x, the initial pressure ratio p_1/p_4 in the shock tube required to produce shocks of given Mach numbers M_s. Tailored conditions are indicated on this graph where appropriate for all possible mixture ratios for which M_T exceeds a value of two.

For a driver pressure of 6000 psia (the maximum pressure used in the R.A.E. shock tunnel) we obtain, with the help of Fig.5, the appropriate ranges of values for the operating stagnation temperature and pressure, T_5 and p_5 respectively. These are shown in Fig.6 and Fig.7. It is of note in Fig.6 that at each shock Mach number M_s the values of T_5 appropriate to the chosen practical range of values of the concentration parameter x are approximately equal, since the corresponding pressure levels p_5 given in Fig.7 are sufficiently high to keep the amount of dissociation and other real-gas processes small. Also in Fig.7 it may be noted that the level of p_5 recovered by tailoring is generally close to driver pressure independently of x. Hence one may optimise Reynolds number by operating the facility in the tailoring mode, which will maintain p_5 at a steady level. Then the mixture concentration x for each nozzle Mach number, M_∞, may be chosen in order to achieve optimisation so that the level of T_5 produced has a value just sufficient to avoid condensation of the test gas in the working section. Moreover as T_5 is reduced, real-gas effects on the thermal properties of the gas will become less pronounced, and calibration techniques based on the assumption of ideal-gas behaviour may be applied when the tunnel is operated at low nozzle Mach numbers.

3.3 Working section conditions for tailored operation

Figs.8, 9 and 10 show the flow pressure, temperature and density which are obtained in the working section for tailored operation with a mixed driver and nozzle Mach numbers, M_∞, of 5, 10 and 15. Also shown on these diagrams are condensation limits calculated from the results in Ref.3.

As was anticipated in the previous section, the effect of variation of the mixture ratio of the driver gas on the ambient pressure level shown in

Fig.8 is not very marked. However owing to the effect of the mixture ratio on temperature level in Fig.9, the change in ambient density (shown in Fig.10) with increasing concentration of N_2 in the mixture (i.e. x decreasing) is very pronounced. As can be seen from Fig.10 at nozzle Mach numbers between 5 and 10, densities of the order of atmospheric density should be possible for values of x between 0·6 and 0·8.

3.4 Reynolds number for tailored conditions

Fig.11 shows the calculated Reynolds number per foot obtained in the working section for various nozzle Mach numbers, M_∞, and for tailored operation. A large increase in Reynolds number is predicted with decrease in x, and values of Reynolds number per foot around 10 million should be available at nozzle Mach numbers in the range between 5 and 10. At nozzle Mach numbers above this range the maximum Reynolds number will be limited by the necessity of maintaining the reservoir temperature above the level at which condensation occurs in the flow in the working section[3].

The significance of Reynolds-number capability in relation to studies of transition is illustrated in Fig.12, where Fig.11 is re-presented in terms of the ratio of the wall temperature of a model in the working section to the total temperature applicable in each case. Since models of over 1 foot in length can be accommodated in the R.A.E. shock tunnel, Fig.12 suggests that for nozzle Mach numbers of between 5 and 10 it should be possible to study natural transition with model Reynolds numbers up to 10 million for highly cooled walls such that the ratio T_W/T_5 (or T_W/T_r) has a value of about 0·2.

3.5 Working section conditions for off-tailored operation

In Figs.13 to 22 working section conditions are given in terms of the primary shock-wave Mach number, M_s, for a mixture driver pressure p_4 of 6000 psia (facility maximum). Results are quoted for fixed nozzle Mach numbers, M_∞, of 5, 10 and 15 and the conditions for tailored operation are shown on each figure. Condensation limits are indicated as previously. As before, the calculations have been made for a test gas of nitrogen, but if it is air the results will still indicate trends correctly. Although theoretically the optimum running-time of an ideal shock tube is obtained when M_s has the value M_T, corresponding to tailored operation, in practice non-tailored operation may be necessary in order to minimise certain effects,

for example premature cooling of the test gas due to contamination by the cold driver gas (see section 4.1). A compromise of this sort can only be reached by calibrating the facility.

4 SOME CAUSES OF IMPAIRMENT OF FACILITY PERFORMANCE

As mentioned before in section 3 the calculations presented are based on the assumption of an ideal flow in the shock tube. In practice calibration of the facility is necessary to make allowances on test conditions for the effect of significant deviations from ideal flow. A brief discussion is now given of some of the principal causes of non-ideal performance in shock tunnels.

4.1 Flow cooling due to shock-wave bifurcation

Premature cooling of the nozzle reservoir gas (flow region 5, Fig.1) may occur due to bifurcation of the reflected shock wave when it interacts with the boundary layer on the shock tube wall. This well known effect[4,5] is attributed to cold driver gas which enters through the foot of the bifurcation to surround the heated gas in the channel. Recent experimental work by Allan[6] has shown that this phenomenon is important in reflected-shock tunnels where the boundary layer is almost entirely turbulent.

Experimental and theoretical work by Mark[7], Davies[4] and others has indicated the critical values of the primary-shock Mach number above which bifurcation is expected. For a reflected shock in a nitrogen test gas this Mach number is about 1·8, and so some bifurcation will occur for all the conditions involving a mixed driver which are considered in this Report. However, Davies' analysis[4] of the reflected shock after transmission into the driver gas has shown that the bifurcation will only be supported above a second critical Mach number, which is of the order of the tailoring Mach number. Below this value the bifurcated foot is expected to diminish rapidly and the contamination of the reservoir gas should not be serious.

In practice, however, in the reflected-shock tunnel the extent of premature cooling can be detected during calibration by heat-transfer measurements on models in the working section[8] and its overall significance thereby assessed.

4.2 Other factors influencing shock-tube performance

Attenuation of the primary shock-wave and the cooling of the flow by the walls of the tube will affect the primary flow[9,10] in the shock tube. In addition, compressibility effects and isotopic changes in the high-pressure

hydrogen driver gas[11] can also have some influence on shock-tube performance. Other factors[9,10] such as interface combustion, if air is used as the test gas, contact surface instability and mixing in the contact region (affected by the diaphragm bursting process) further complicate the 'ideal' picture of shock-tube flow.

4.3 Application of theoretical results under actual flow conditions

Owing to the effects listed above, the performance of the facility will fall short of that estimated. In particular in order to obtain a primary shock of a specified Mach number in the channel the shock tube has in general to be 'overdriven', and sometimes a driver pressure of about twice the theoretical estimated value is actually required[8].

However, even when departures from the theoretically assumed flow model are significant or when the driver pressure p_4 is not equal to the value of 6000 psia (facility maximum) assumed in the calculations, use may still be made of the result presented in this Report. To do this an 'effective' value of p_4 must be found from Fig.5 using the measured value of M_s and the known values of x and p_1. The pressure ratios given in Figs.7, 8, 14, 15 and 16 may then be used directly with p_4 now equal to its effective value. The temperature values given in Figs.6, 9 and 13 may also be used as before, since pressure adjustment will have only a slight effect on these temperature plots. However, the values for the flow density given in Figs.10, 17, 18 and 19 and for the Reynolds number per foot in Figs.11, 12, 20, 21 and 22, which are all directly proportional to p_4, must be scaled by a factor equal to the ratio of the effective value of p_4 to the original driver pressure of 6000 psia used in the calculations. In addition to this, when the results for the ambient pressure level in the working section have to be corrected in the manner described, the condensation limits shown will be altered correspondingly. It is not possible to indicate precisely how these limits will vary, but the trend is that the range of condensation-free flow will be extended in Figs.8, 9, 10, 11, 12, 15, 16, 18, 19, 21 and 20 as long as p_4 effective is less than 6000 psia and vice versa. Hence for the R.A.E. shock tunnel, where p_4 effective is always less than the facility maximum driver pressure of 6000 psia[8], the condensation limits given in the results will be pessimistic.

4.4 Real-gas effects on working section Mach number

Fig.23 shows for inviscid flow of N_2 in thermodynamic equilibrium the relationship between the primary shock Mach number, M_s, and the working section

Mach number, M_∞. Values of M_∞ have been obtained for each value of the area ratio A/A*, which is fixed for each nozzle and is equal to the ratio of the cross-sectional area of the working section, A, to the throat area, A*. As M_s increases from 2 to about 3 the reservoir enthalpy rises to a level where real-gas thermodynamic effects begin to become appreciable and it is found that the Mach number in the working section, M_∞, begins to diminish for constant A/A* as a result of this. At even higher enthalpies, such that the assumption of thermodynamic equilibrium throughout the nozzle expansion is no longer valid, the general picture shown in Fig.23 will become further complicated.

These results are further illustrated in Fig.24 for the area ratios appropriate to existing nozzles for the R.A.E. 15" reflected-shock tunnel. Hence we see that only at the lower shock Mach numbers, M_s, for low total-enthalpy conditions can a nominal value for the working section Mach number, M_∞, be assumed.

5 CONCLUSIONS

(1) Use of the R.A.E. 15" shock tunnel in the dual role of a high Reynolds number facility and high-enthalpy facility is possible by the application of a mixed driver technique.

(2) Calculations based on ideal shock-tube performance indicate that a mixed driver of hydrogen and nitrogen could be used in the reflected-shock tunnel with a test gas of nitrogen or air to obtain improved Reynolds numbers in the working section. At the facility maximum driver pressure of 6000 psia the Reynolds numbers of up to 10 million per foot obtained should be sufficient to cause natural transition on a model tested at free-stream Mach numbers in the range between 5 and 10.

(3) When operated as a low-enthalpy facility, calibration of this tunnel at the lower nozzle Mach numbers becomes easier, since calculations of the flow and selection of measurement techniques can be based on the assumption of an ideal gas. Also the density in the working section then approaches the level of atmospheric density and flow visualisation is thereby much improved.

(4) Because the shock-tube performance is inevitably non-ideal, calibration will be necessary in order to determine the initial conditions which will produce optimum duration of both the reservoir pressure and temperature, as this may be expected to result in maximum running time of the facility.

Appendix

FORMULAE ASSOCIATED WITH REFLECTED-SHOCK TUNNEL CALCULATIONS FOR MIXED $H_2 : N_2$ DRIVER GAS WITH N_2 (OR AIR) AS TEST GAS

The particle (or molecule) concentration parameter x is defined by the ratio of the number of molecules of H_2 to the number of molecules of both H_2 and N_2 in a unit volume of mixture.

Hence, if $p_i(N_2)$ is the initial pressure of N_2 in the driver before H_2 is added to raise the pressure to the final driver pressure $p_f(= p_4)$, then we have that:

$$x = 1 - \frac{p_i}{p_f} \tag{1}$$

γ_x, the ratio of specific heats for the mixture, is constant at the value of 1·4 appropriate to diatomic molecules.

The mean molecular weight, m_x, and the speed of sound, a_x, for the mixture are then given by:

$$m_x = x\, m_{H_2} + (1 - x)\, m_{N_2} \tag{2}$$

$$\frac{a_x}{\sqrt{T}} \propto \frac{1}{\sqrt{m_x}} \tag{3}$$

Equations (2) and (3) are plotted in Fig.2 using references 12 and 13.

Tailoring condition

In terms of the notation of Fig.1, the condition for tailoring quoted in Ref.14:

$$\frac{a_2}{a_3} = \frac{\gamma_1}{\gamma_4} \left\{ \frac{1 + \left(\frac{\gamma_1 + 1}{2\gamma_1}\right)\left(\frac{p_5}{p_2} - 1\right)}{1 + \left(\frac{\gamma_4 + 1}{2\gamma_4}\right)\left(\frac{p_5}{p_2} - 1\right)} \right\}^{\frac{1}{2}} \tag{4}$$

reduces to:

$$a_2 = a_3 \tag{5}$$

since $\gamma_1 = \gamma_2 = \gamma_3 = \gamma_4$ for an $H_2 : N_2$ mixture driving N_2 (or air).

Applying the standard formulae:

$$a_3 = a_4 - \frac{(\gamma_4 - 1)}{2} u_2, \quad \text{where} \quad u_2 = \frac{2a_1}{(\gamma_1 + 1)} \left(M_s - \frac{1}{M_s} \right) \tag{6}$$

and

$$\frac{a_2^2}{a_1^2} = \left(\frac{p_2}{p_1}\right) \frac{\left[\left(\frac{p_2}{p_1}\right) + \left(\frac{\gamma_1 + 1}{\gamma_1 - 1}\right) \right]}{\left[\left(\frac{\gamma_1 + 1}{\gamma_1 - 1}\right) \left(\frac{p_2}{p_1}\right) + 1 \right]}, \quad \text{where} \left(\frac{p_2}{p_1}\right) = \left\{ \frac{2\gamma_1 M_s^2 - (\gamma_1 - 1)}{(\gamma_1 + 1)} \right\} \tag{7}$$

we obtain by the tailoring condition in equation (5), for each value of x (i.e. $a_x = a_4$), a value for M_s equal to M_T. A plot of this Mach number for tailoring, M_T, is shown in Fig.4.

Initial pressure ratio (p_4/p_1)

For each value of x (i.e. $a_x = a_4$) plots of (p_4/p_1) versus M_s were obtained for Fig.5 using the derived formula:

$$\frac{p_4}{p_1} = \left(\frac{p_2}{p_1}\right) \left[1 - \left\{ \left(\frac{p_2}{p_1}\right) - 1 \right\} \frac{(\gamma_4 - 1)}{(\gamma_1 - 1)} \frac{a_4}{a_1} \left\{ \frac{\left(\frac{\gamma_1 - 1}{2\gamma_1}\right)}{\left(\frac{\gamma_1 + 1}{\gamma_1 - 1}\right)\left(\frac{p_2}{p_1}\right) + 1} \right\}^{\frac{1}{2}} \right]^{-\frac{2\gamma_4}{(\gamma_4 - 1)}} \tag{8}$$

with again from (7):

$$\left(\frac{p_2}{p_1}\right) = \left\{ \frac{2\gamma_1 M_s^2 - (\gamma_1 - 1)}{\gamma_1 + 1} \right\}.$$

Calculations for other regions in the flow of test gas

The shock-tunnel reservoir (region 5) conditions were obtained by using Ref.15.

Working section conditions (region ∞) were derived using Ref.16 together with Ref.17 when ideal-gas conditions were appropriate.

SYMBOLS

T	ambient temperature (°K)
a	speed of sound in gas (ft/sec)
p	ambient pressure (psia)
ρ/ρ_o	ambient density ratioed to atmospheric density (i.e. amagat units)
γ	ratio of specific heats
M_s	Mach number of primary shock wave
M_T	Mach number of primary shock wave for tailored condition
M_∞	exit Mach number of nozzle, i.e. free-stream Mach number in the working section
T_W	wall temperature for a model in the working section
T_r	recovery temperature for a model in the working section
A/A^*	cross-sectional area ratio for working section to throat conditions for nozzle
t	time
x'	distance along shock-tube from main diaphragm
Re/ft	Reynolds number per foot in the working section
m_{H_2}	molecular weight of H_2
m_{N_2}	molecular weight of N_2
m_x	mean molecular weight of $H_2 : N_2$ mixture for particle (molecular) concentration x
x	particle (or molecular) concentration of $H_2 : N_2$ mixture (see Appendix for definition)
a_x $(= a_4)$	speed of sound in mixture (ft/sec)
$p_i(N_2)$	initial pressure of N_2 in driver (psia)
$p_f(H_2 : N_2)(= p_4)$	final driver pressure for $H_2 : N_2$ mixture (psia)

Subscripts

1, 2, 3, 4, 5, ∞ for definition of flow regions, see Fig.1

REFERENCES

No.	Author	Title, etc.
1	L. H. Townend S. G. Cox	Base-burning and 'near wake' combustion. (Remarks on a paper by W. C. Strahle.) Both presented at 12th International Combustion Symposium, Poitiens, July 1958
2	J. F. W. Crane J. G. Woodley	Unpublished Mintech Report
3	J. F. W. Crane R. J. Marshall	Air condensation effects measured in the R.A.E. 7 inch x 7 inch hypersonic wind tunnel. A.R.C. R & M 3511 (1966)
4	L. Davies	The interaction of the reflected shock with the boundary layer in a shock tube and its influence on the duration of hot flow in the reflected-shock tunnel. Parts I and II. Part I A.R.C. C.P. 880 (1965) Part II A.R.C. C.P. 881 (1965)
5	L. Davies J. L. Wilson	The influence of shock and boundary layer interaction on shock tube flows. A.R.C. 29064 (1967)
6	J. W. Allan	An experimental study of the interaction between the reflected shock wave and a turbulent boundary layer in a shock tube. R.A.E. Technical Report 68089 (A.R.C. 30788) (1968)
7	H. Mark	The interaction of a reflected shock wave with the boundary layer in a shock tube. NACA TM 1418 (1958)
8	S. G. Cox	Unpublished Mintech Report

REFERENCES (CONTD)

No.	Author	Title, etc.
9	J. N. Bradley	Shock waves in chemistry and physics. Methuen & Co, Ltd., (1962)
10	A. G. Gaydon I. R. Hurle	The shock tube in high temperature chemical physics. Chapman and Hall Ltd (1963)
11	L. Davies L. Pennelegion P. Gough K. Dolman	The effects of high pressure on the flow in the reflected-shock tunnel. A.R.C. C.P.730 (1963)
12	C. H. Lewis C. A. Neel	Specific heat and speed of sound data for imperfect nitrogen. AEDC - TDR-64-114 (1964)
13	C. H. Lewis E. G. Burgess, III	Charts of normal shock wave properties in imperfect nitrogen. AEDC - TOR-64-104 (1964)
14	L. Pennelegion P. J. Gough	The change in shock-tunnel tailoring Mach number due to driver gas mixtures of helium and nitrogen. A.R.C. [illegible] & M 3398 (1963)
15	L. Bernstein	Tabulated solutions of the equilibrium gas properties behind the incident and reflected normal shock-wave in a shock-tube. I - Nitrogen II - Oxygen. A.R.C. C.P.6[illegible]6 (1961)
16	L. Bernstein	Equilibrium real-gas performance charts for a hypersonic shock-tube wind-tunnel employing nitrogen. A.R.C. C.P.6[illegible] (1961)
17	Ames Research Staff	Equations, tables and charts for compressible flow. NACA Report 1135 (1953)

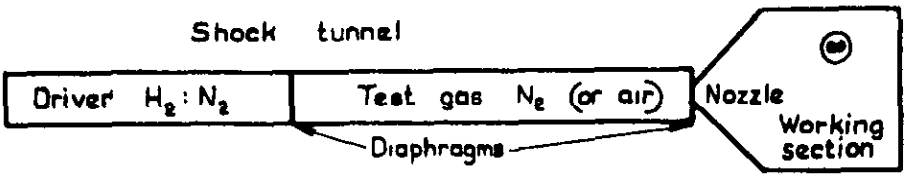

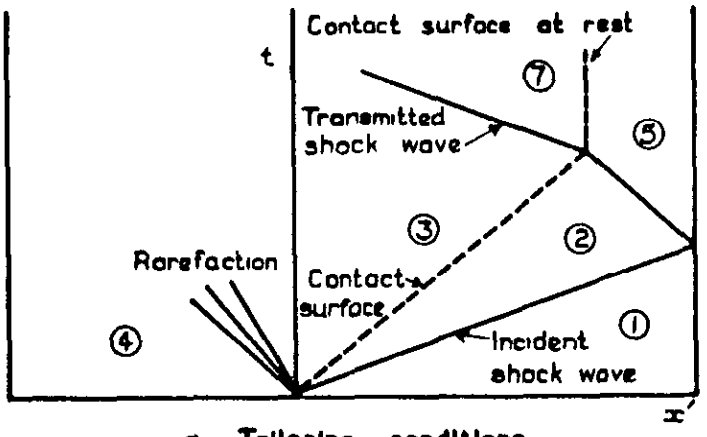

a Tailoring – conditions

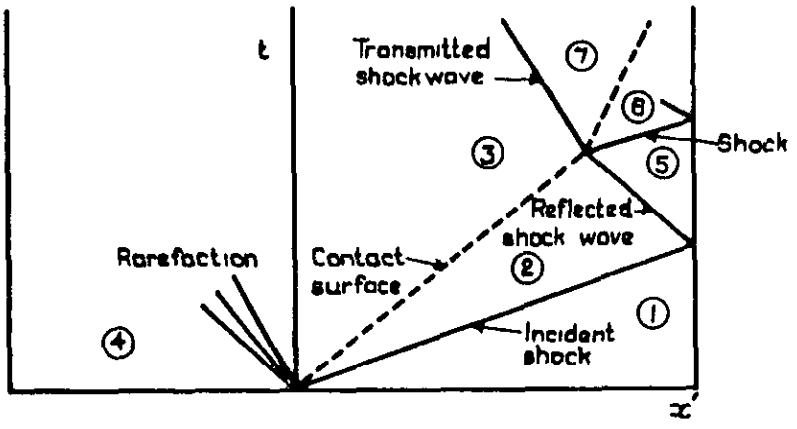

b Over-tailored conditions

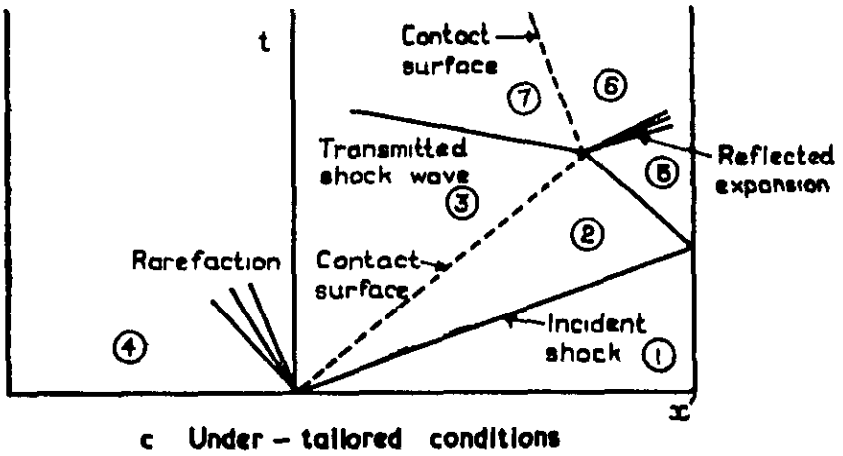

c Under – tailored conditions

Fig. 1 a-c Notation for conditions in a reflected-shock tunnel

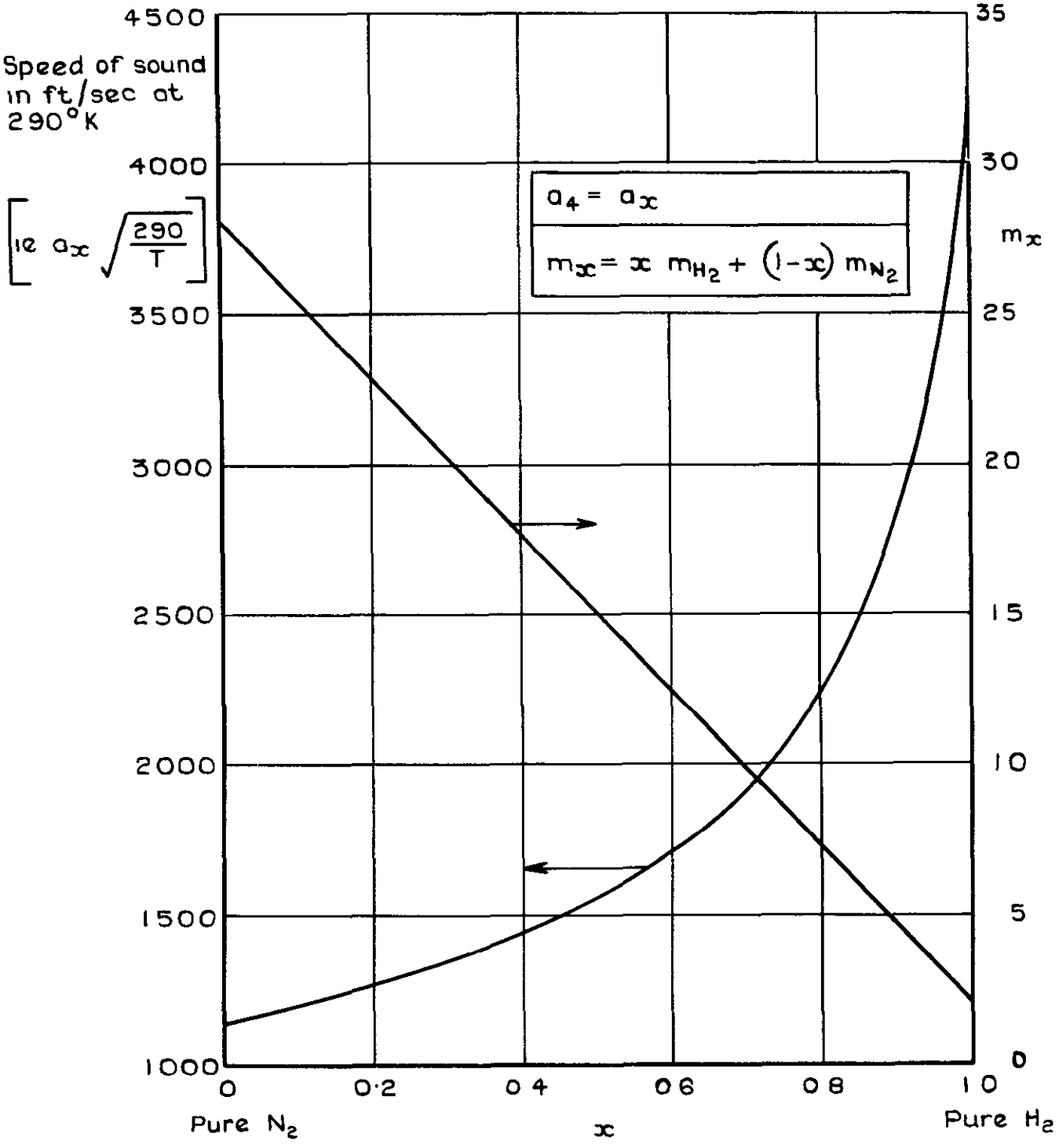

Fig. 2 Mean molecular weight, m_x, and speed of sound, a_x, for $H_2 : N_2$ gas mixture versus particle concentration parameter, x (ie molecules H_2/molecules in mixture $H_2 : N_2$)

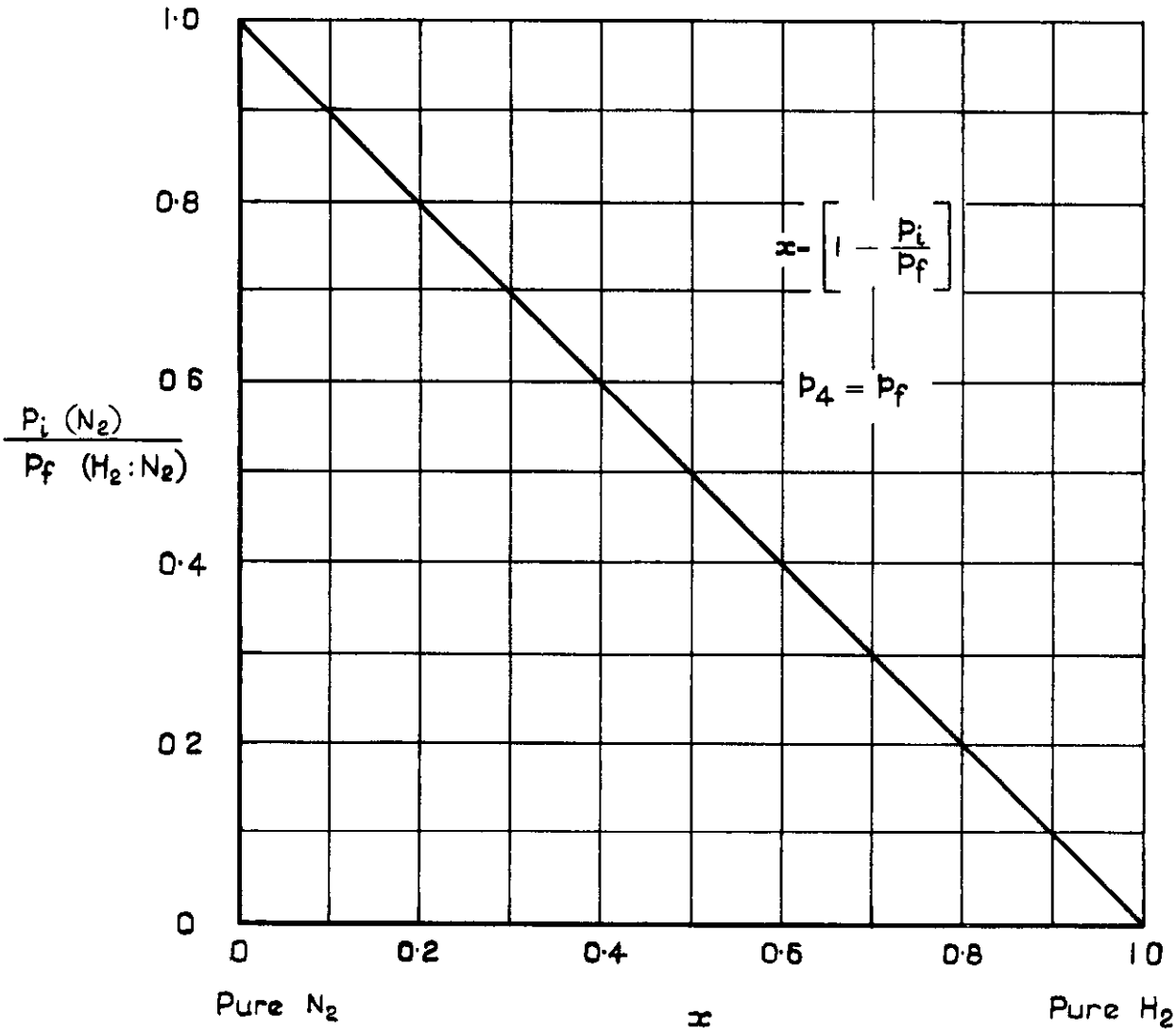

Fig. 3 Ratio of initial pressure of N_2 in driver, p_i, to final driver pressure of $H_2 : N_2$ mixture, p_f, versus particle concentration parameter, x. (See Fig. 1)

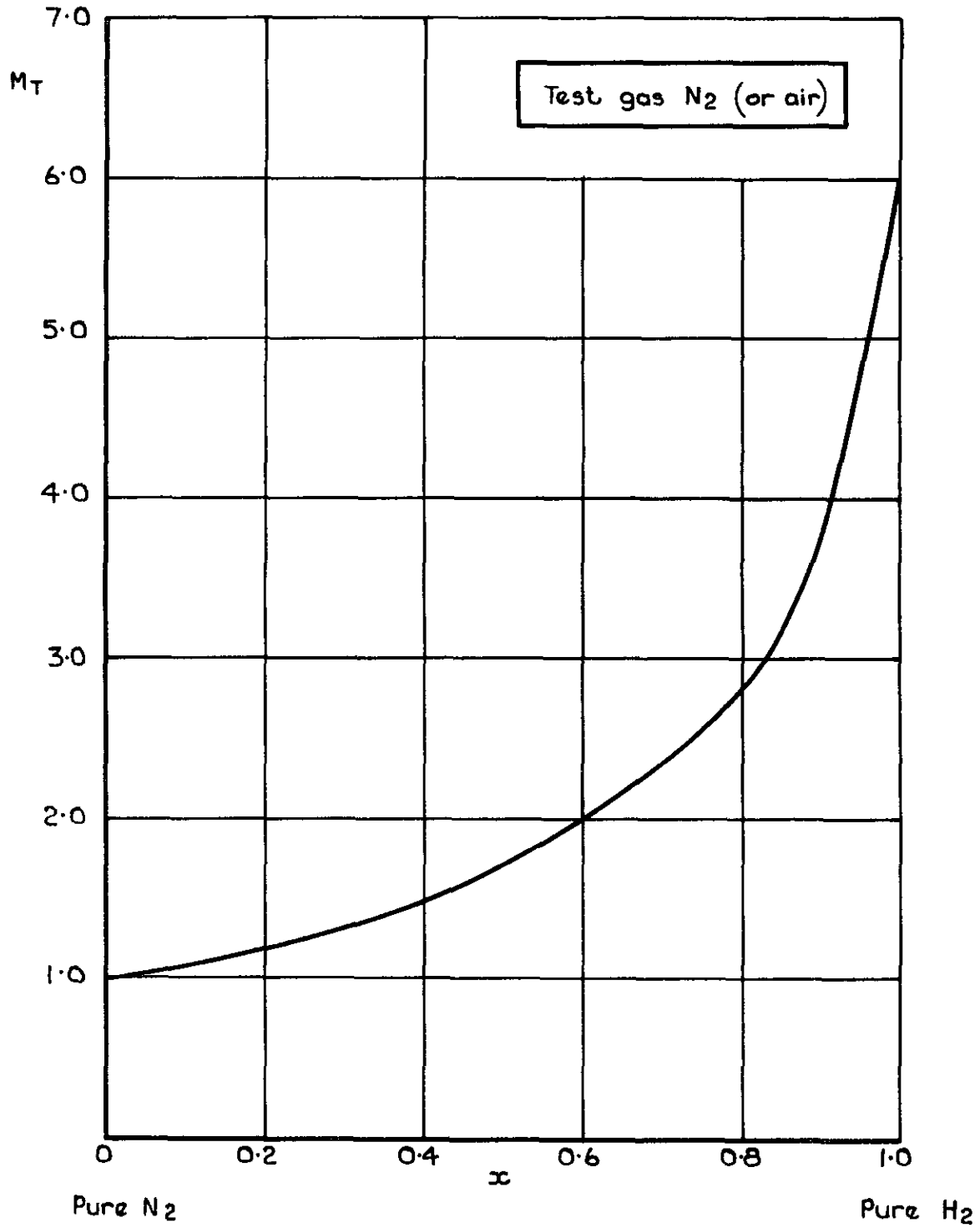
7·0
M_T
6·0
5·0
4·0
3·0
2·0
1·0
Test gas N_2 (or air)
0
0·2
0·4
0·6
0·8
1·0
x
Pure N_2
Pure H_2

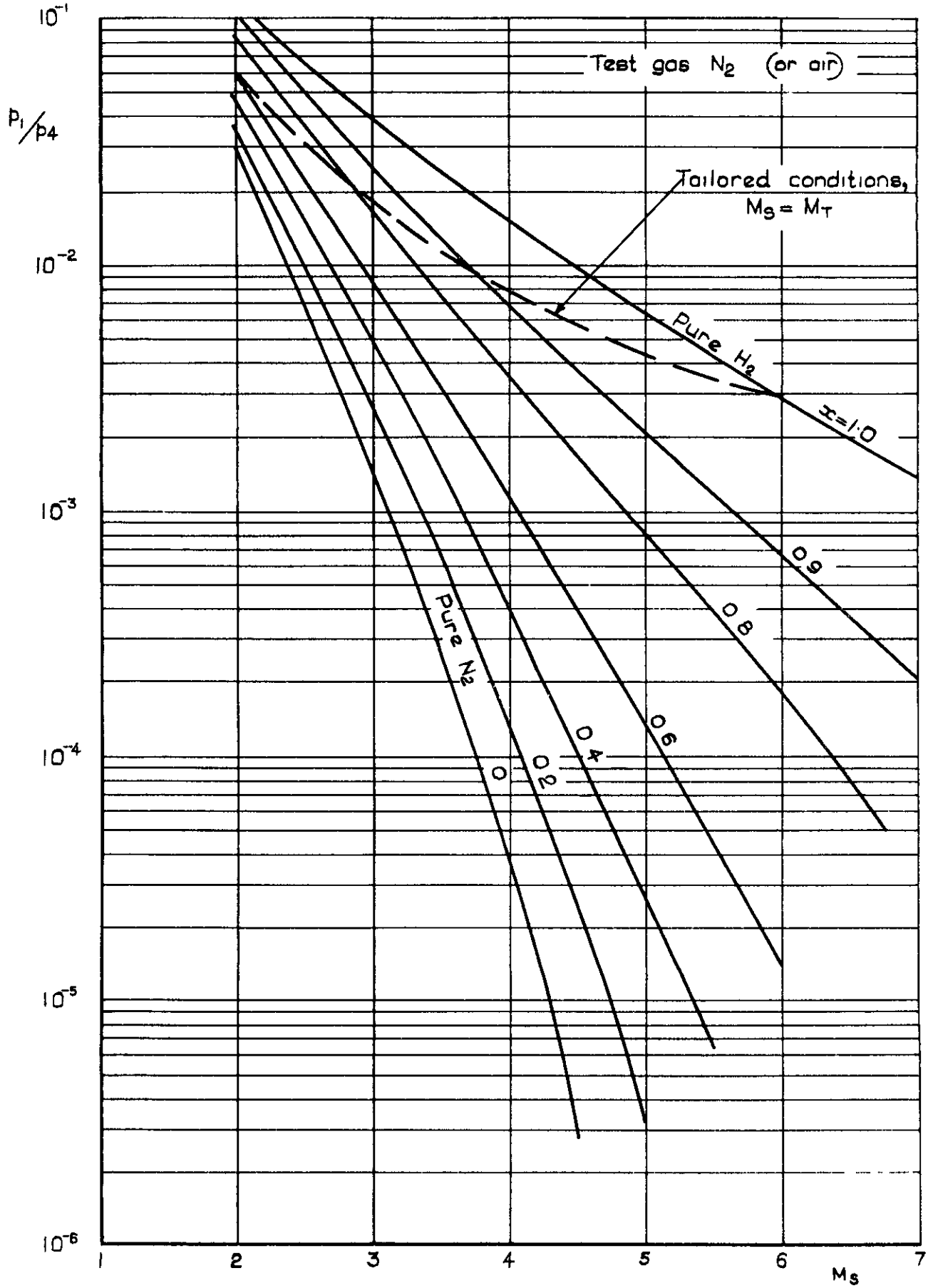

Fig. 5 Ratio of initial channel pressure of N_2, p_1, to final driver pressure, p_4, versus shock Mach number, M_S, for various values of the particle concentration parameter, x.

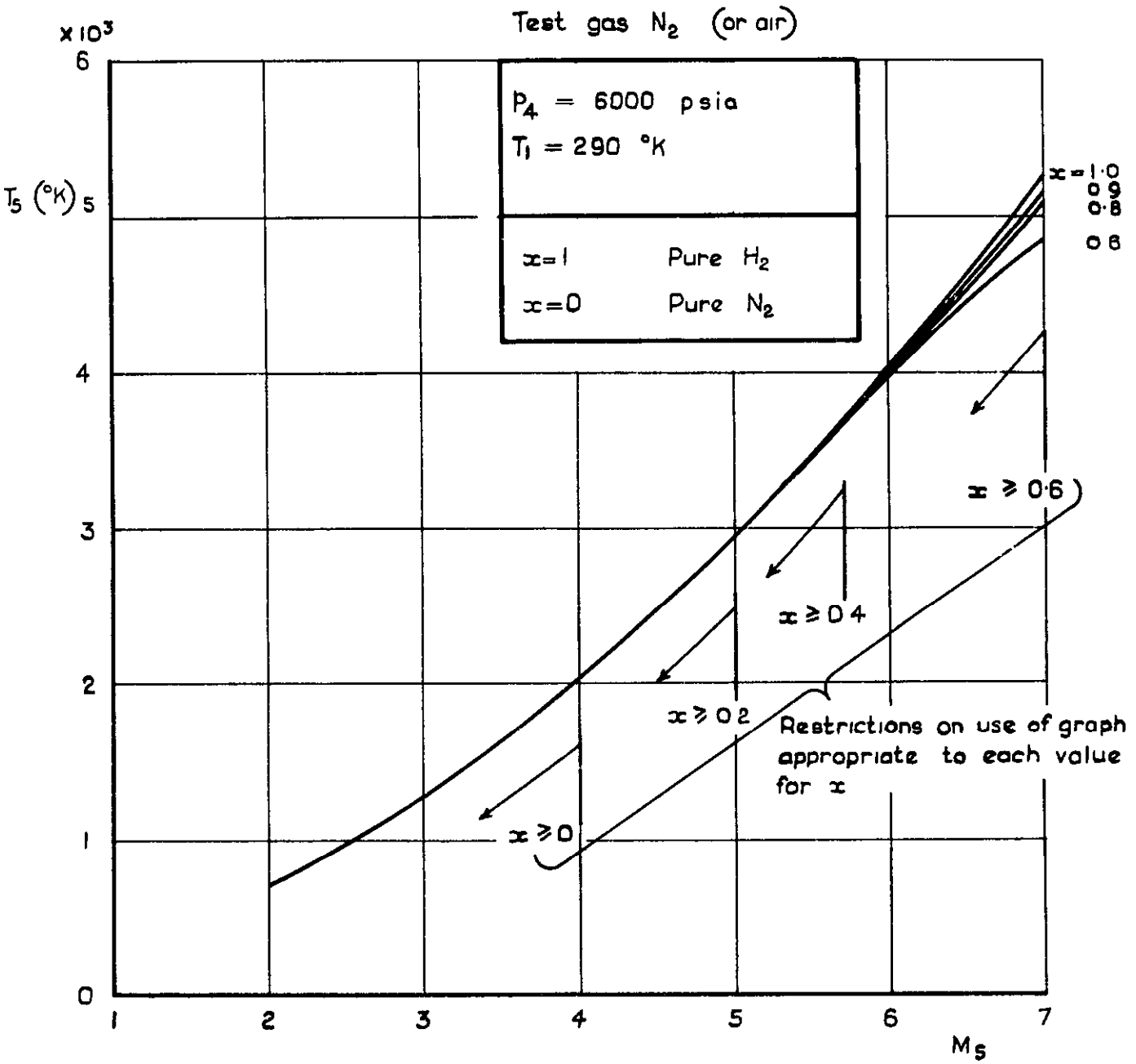

Fig. 6 Reflected-shock temperature, T_5, versus incident-shock Mach number, M_S, for the appropriate ranges of the particle concentration parameter, x.

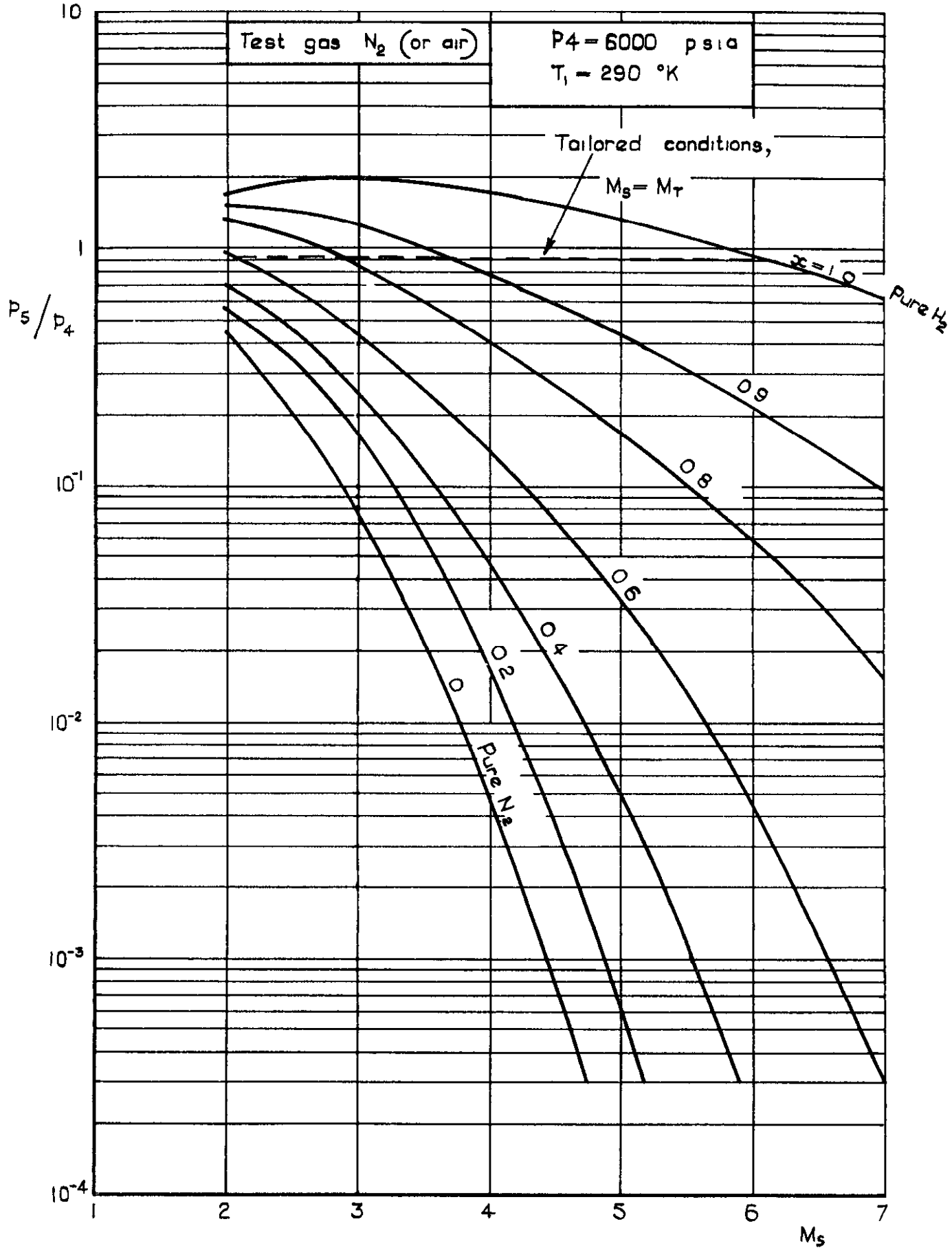

Fig. 7 Ratio of reflected-shock pressure, p_5, to driver pressure, p_4, versus incident-shock Mach number, M_S, for values of the particle concentration parameter, x.

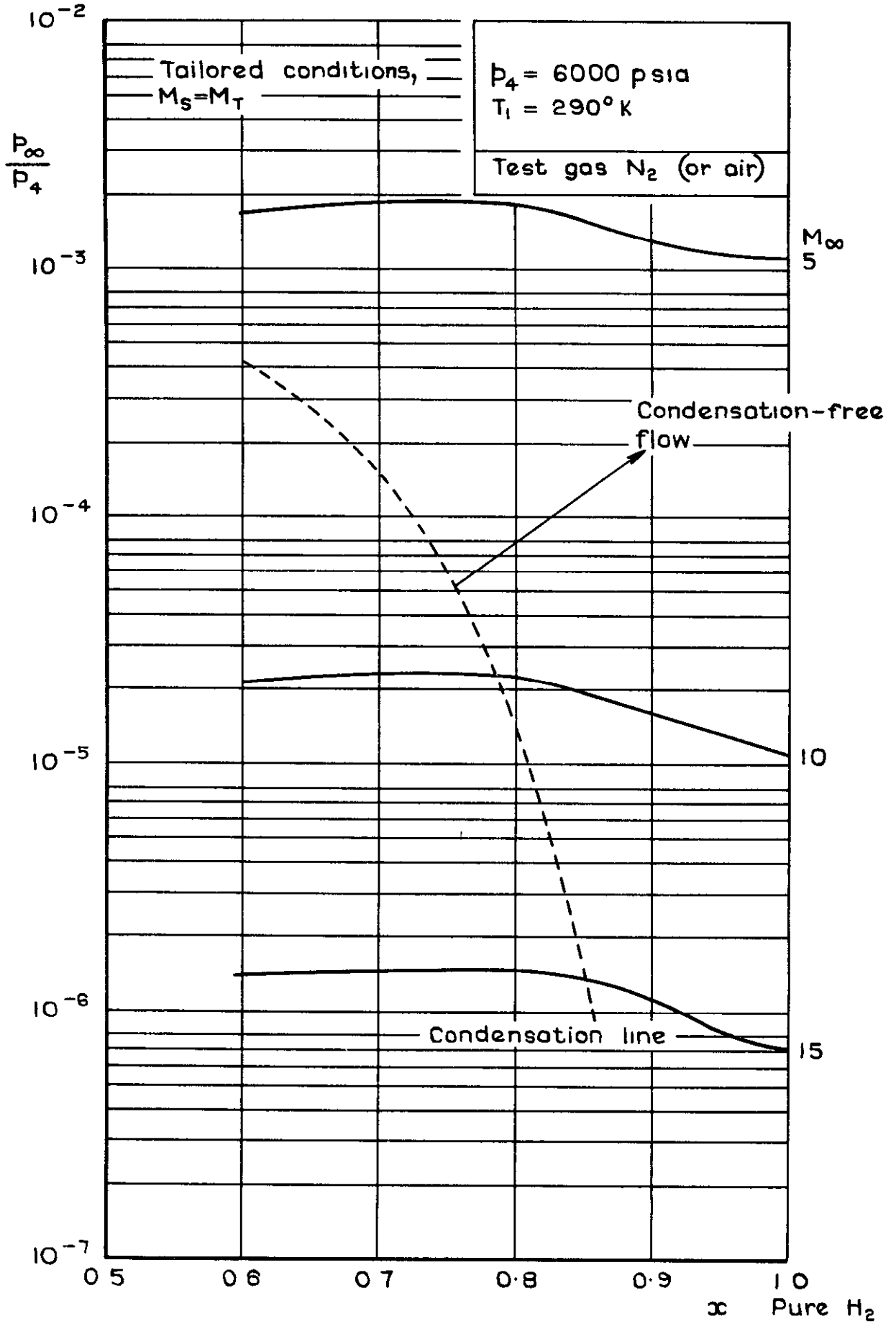

Fig. 8 Ratio of working section pressure, p_∞, to driver pressure, p_4, versus particle concentration parameter, x, for tailored conditions for various nozzle Mach numbers, M_∞

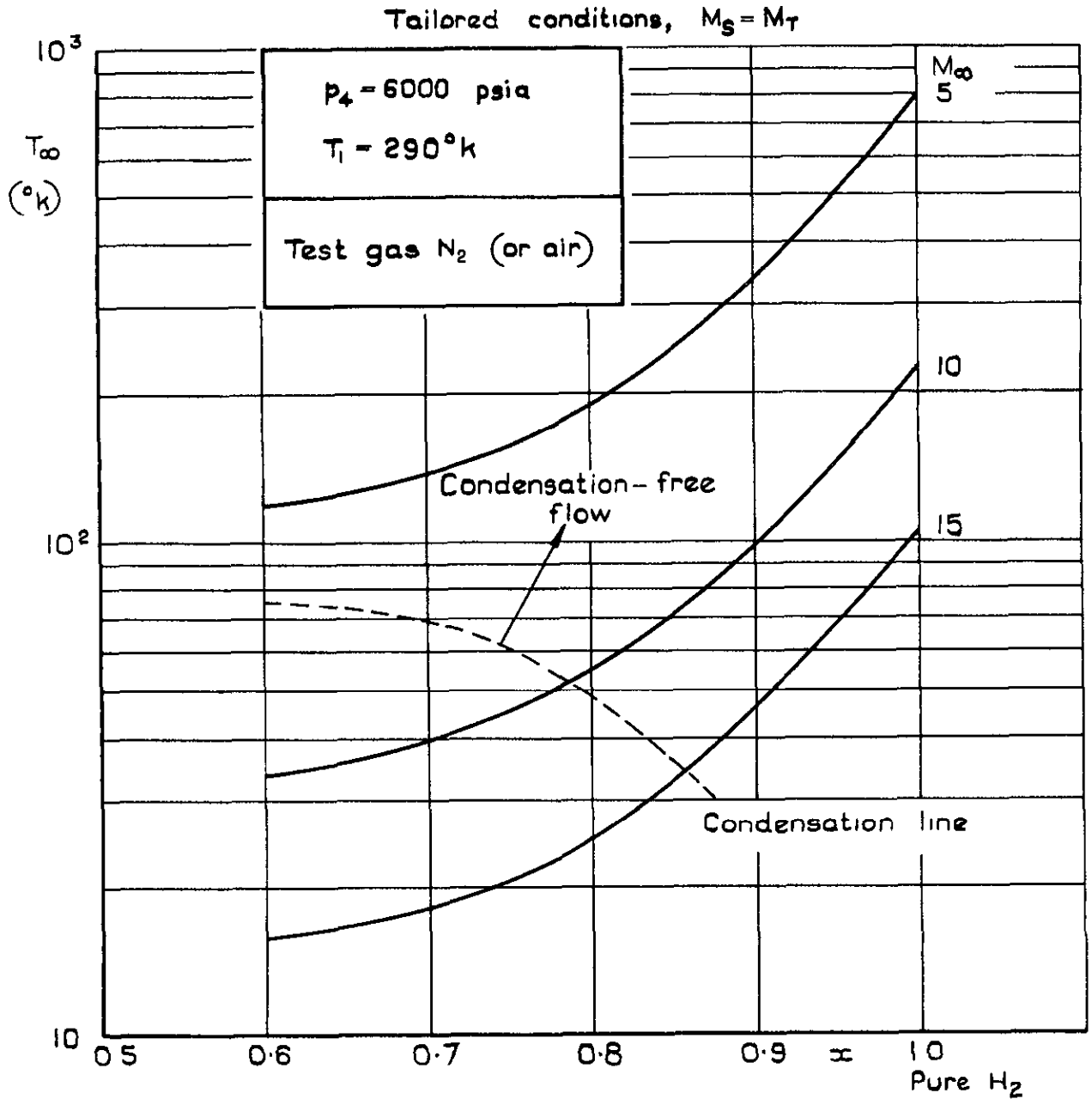

Fig. 9 Ambient temperature, T_∞, in the working section versus particle concentration parameter, x, for tailored conditions, for various nozzle Mach numbers, M_∞

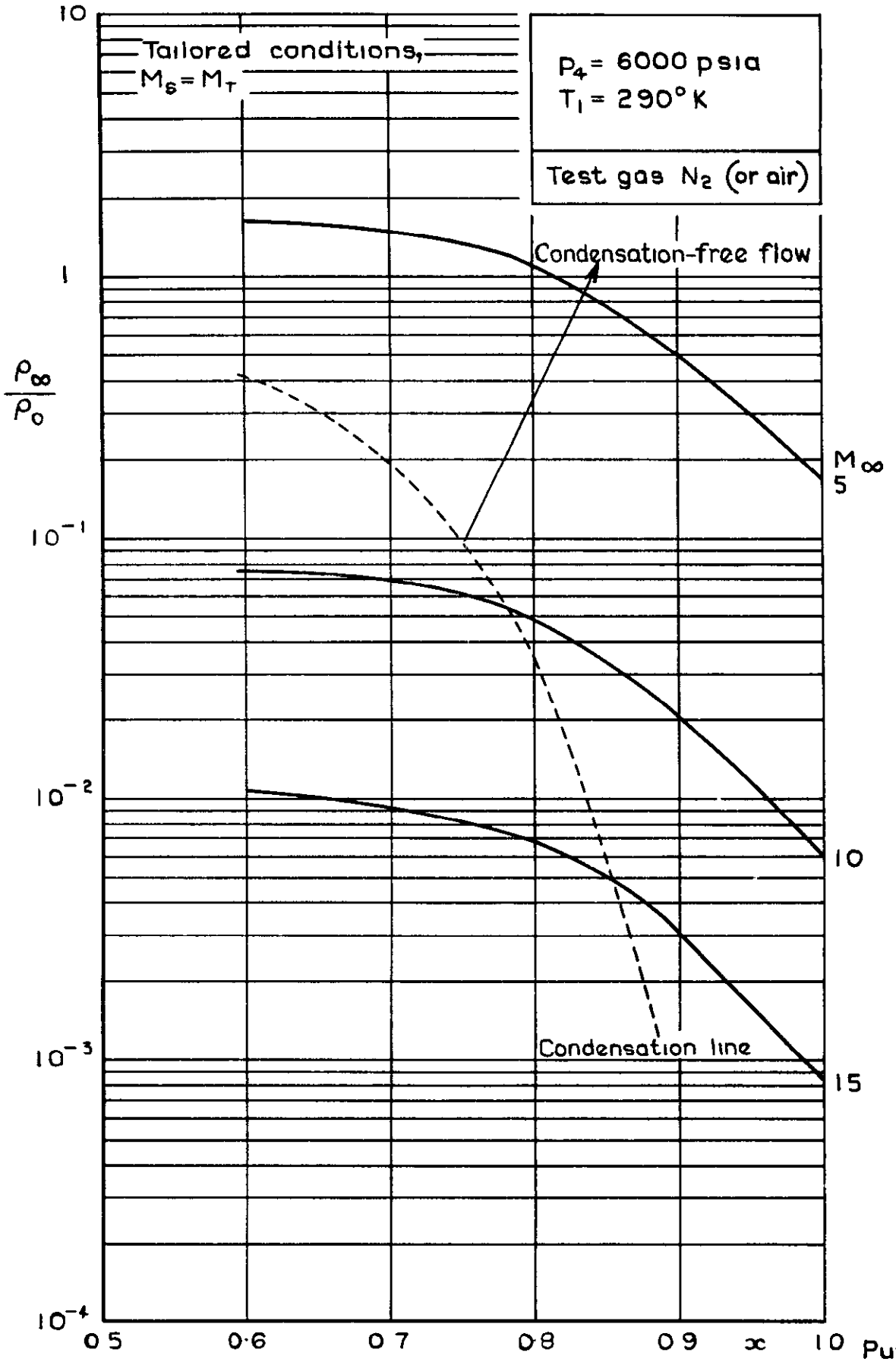

Fig. 10 Ratio of density in the working section, ρ_∞, to atmospheric density, ρ_0, for tailored conditions versus particle concentration parameter, χ, for various nozzle Mach numbers, M_∞

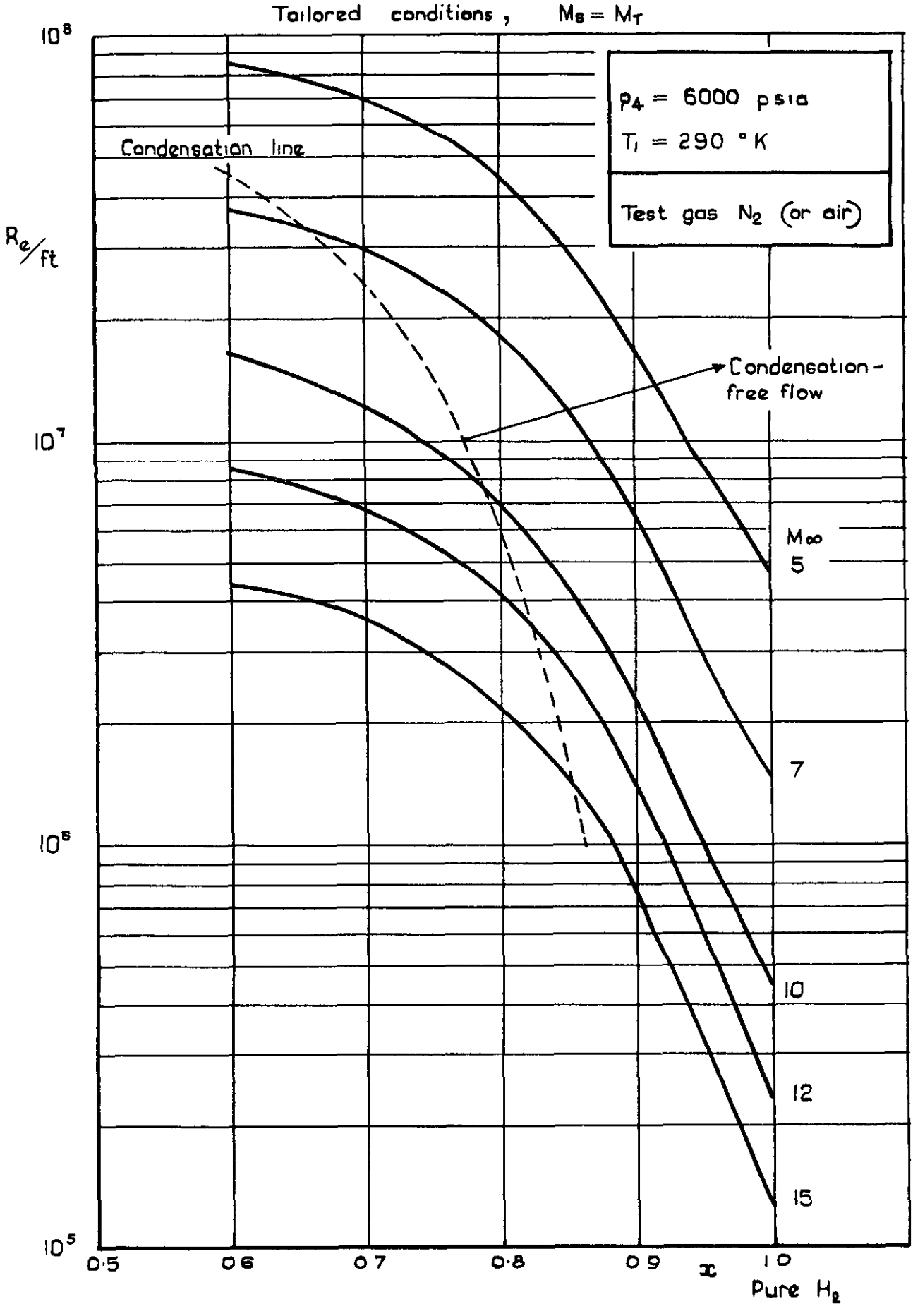

Fig. 11 Reynolds number per foot in the working section versus particle concentration parameter, x, for tailored conditions, for various nozzle Mach numbers, M_∞

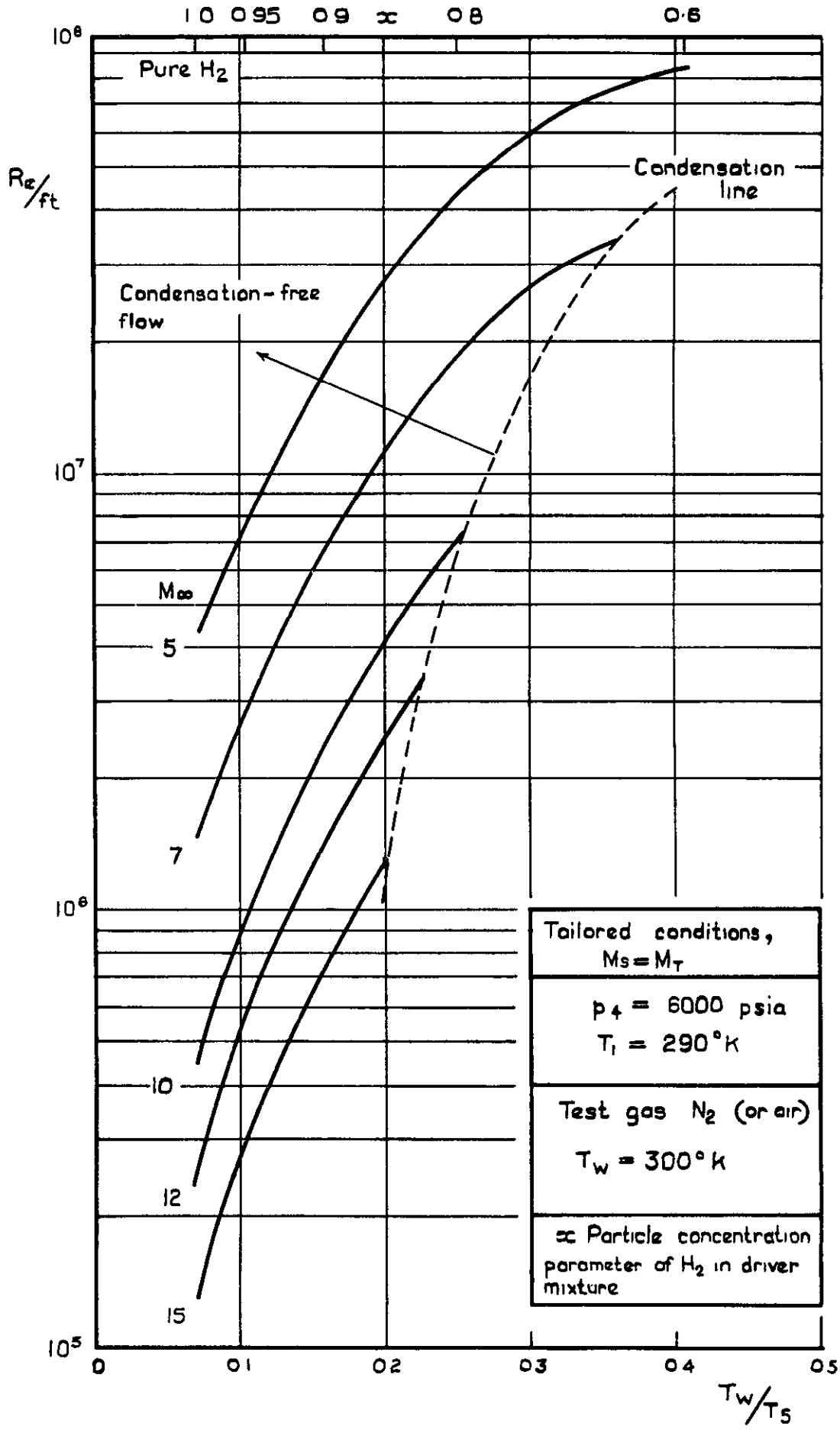

Fig. 12 Reynolds number per foot in the working section versus the ratio of a typical wall temperature, T_w, to total temperature, T_5, for various nozzle Mach numbers, M_∞

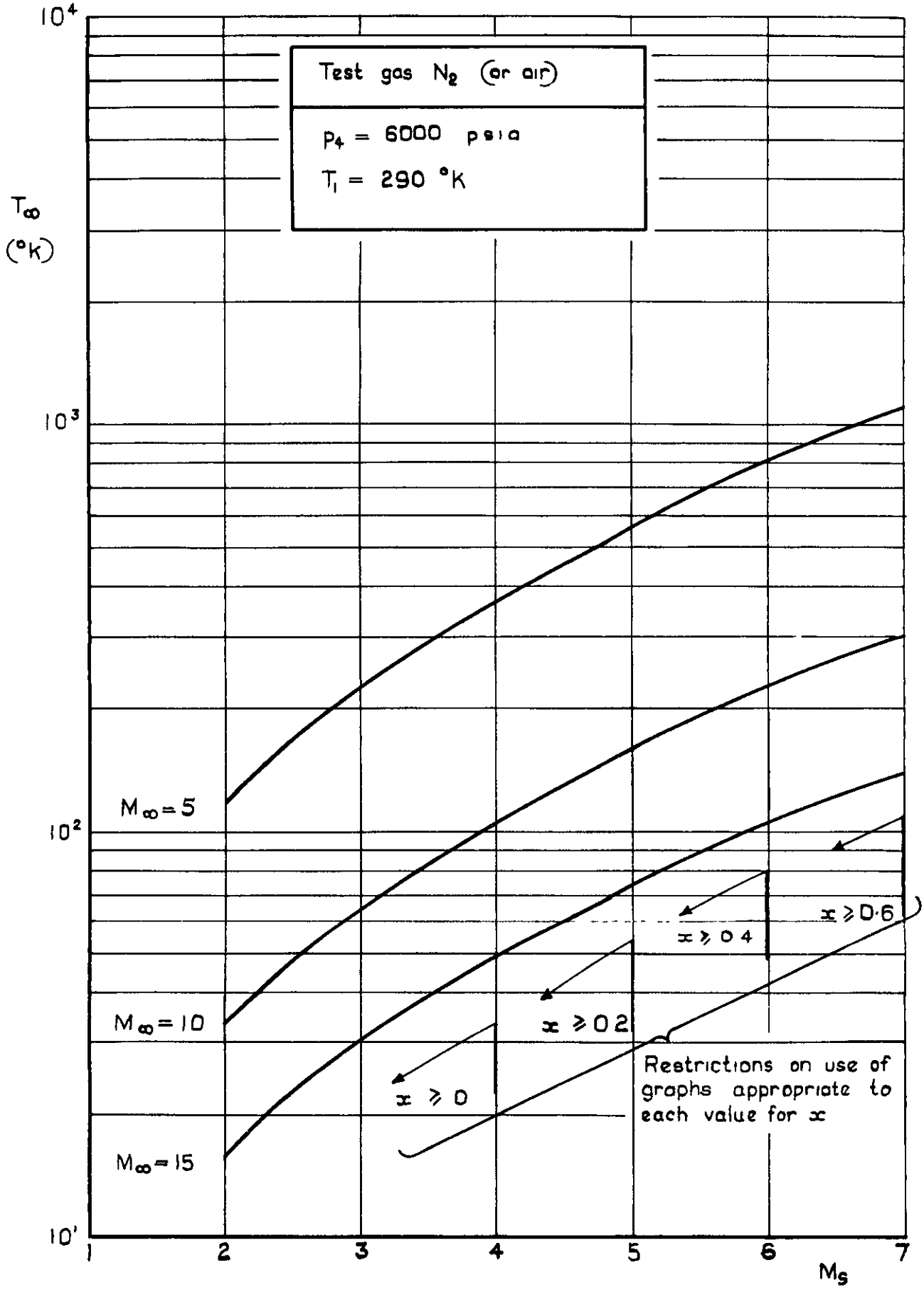

Fig. 13 Ambient temperature, T_∞, versus incident – shock Mach number, M_S, for nozzle Mach numbers, M_∞, of 5, 10 and 15

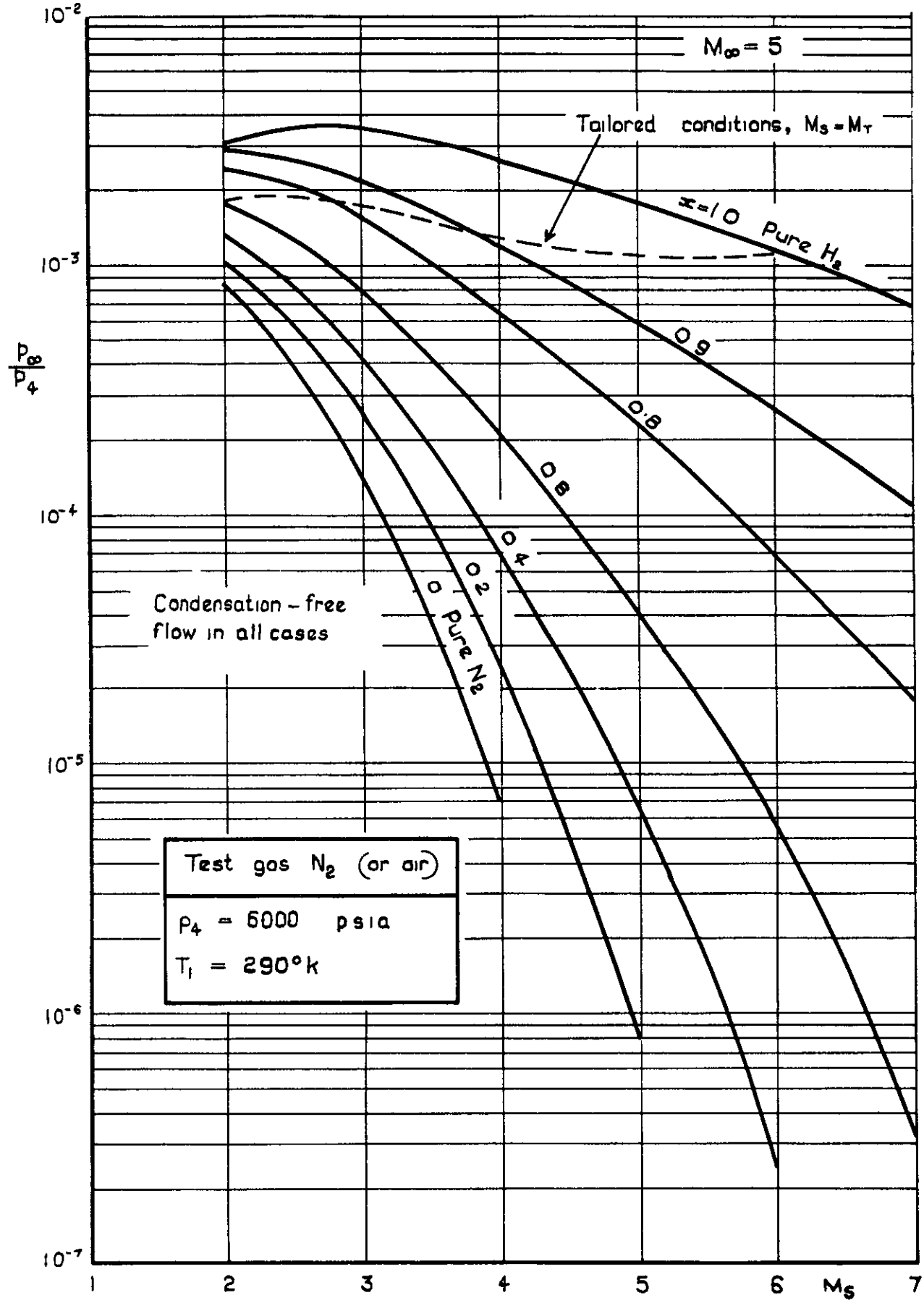

Fig 14 Ratio of free-stream pressure, p_∞, in the working section to driver pressure, p_4, versus incident-shock Mach number, M_s, for various values of the particle concentration parameter, x. ($M_\infty = 5$)

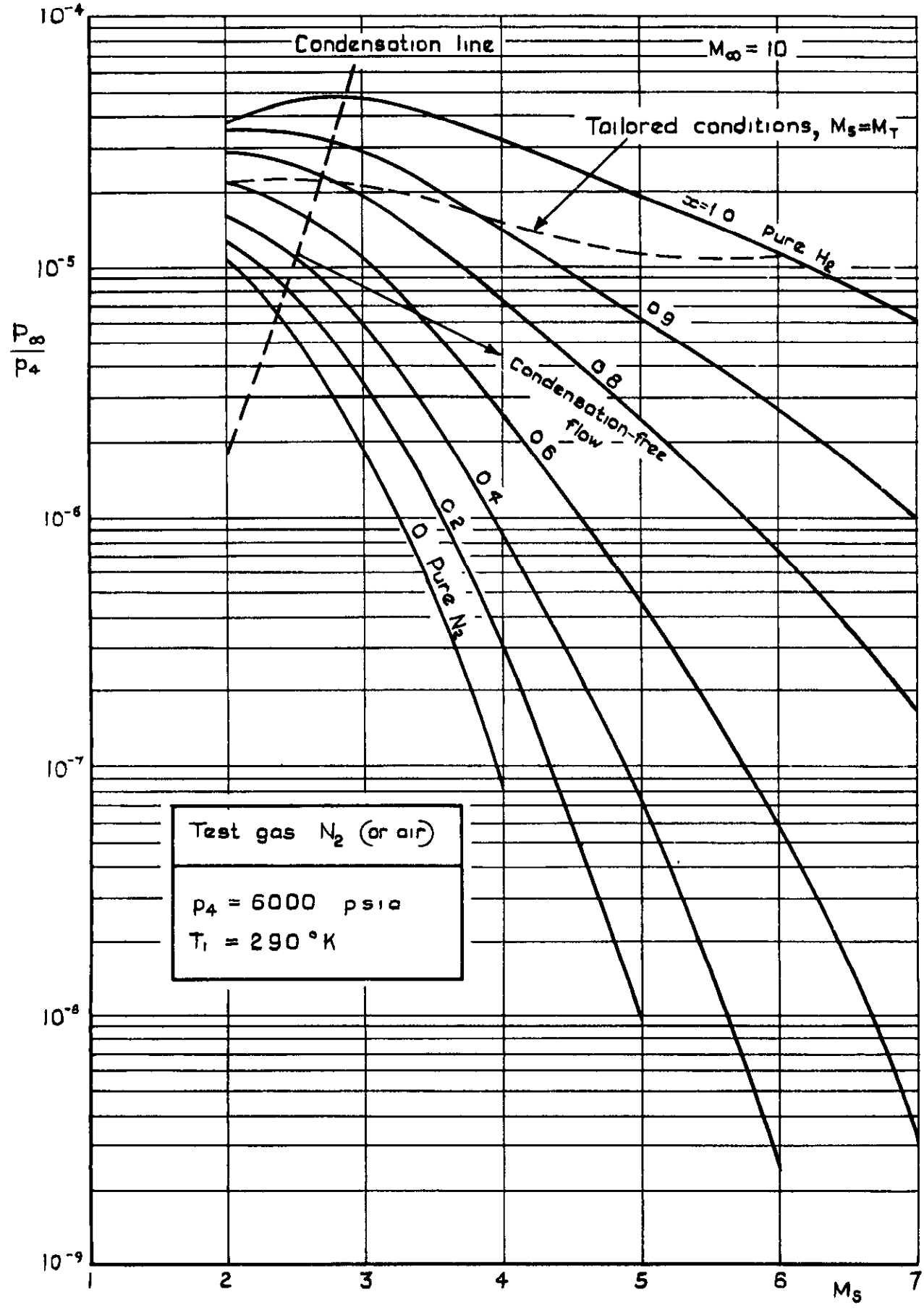

Fig. 15 Ratio of free-stream pressure, p_∞, in the working section to driver pressure, p_4, versus incident-shock Mach, M_S, for various values of the particle concentration parameter, x. ($M_\infty = 10$)

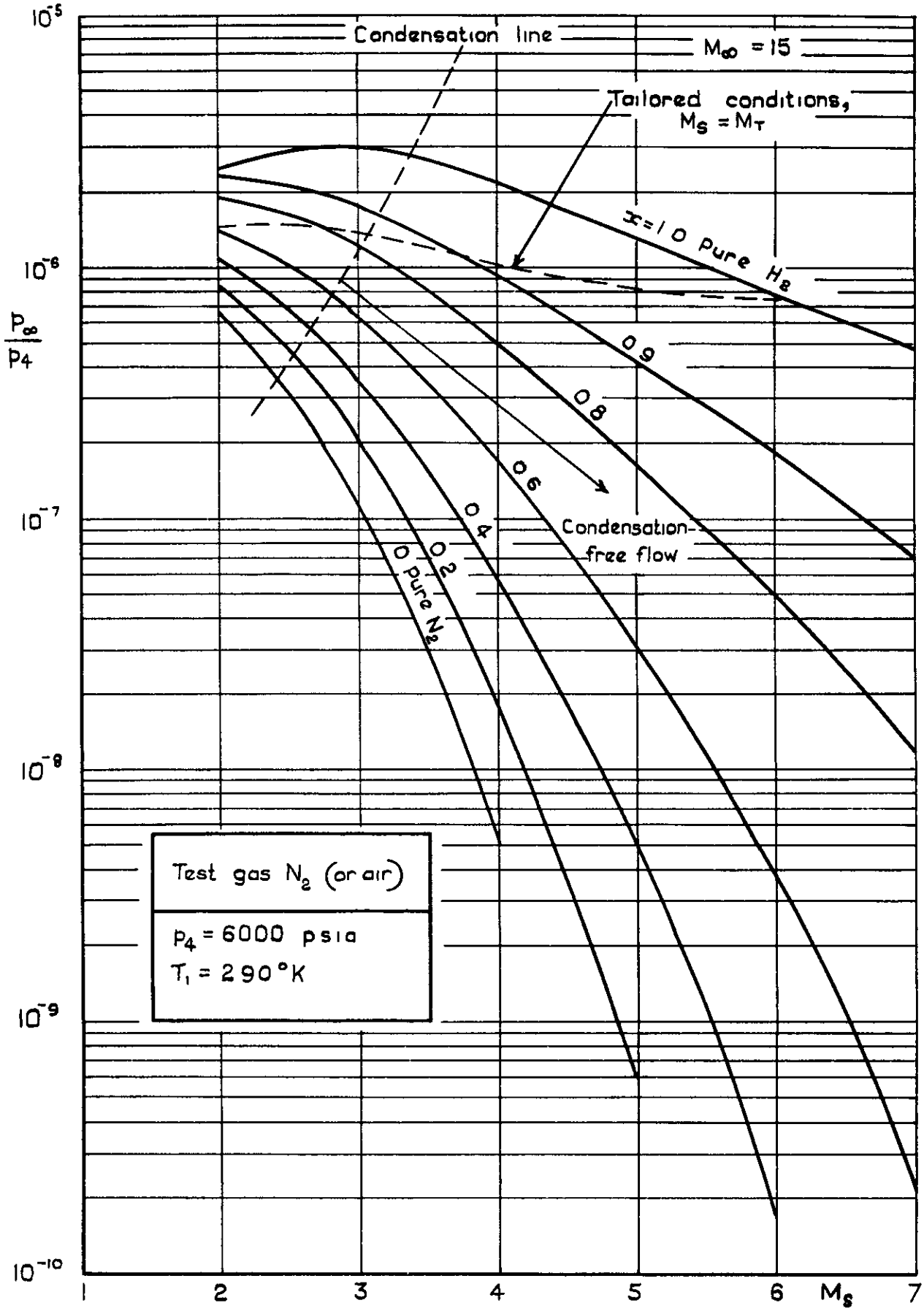

Fig. 16 Ratio of free-stream pressure, p_∞, in the working section to driver pressure, p_4, versus incident-shock Mach number, M_S, for various values of the particle concentration parameter, x. ($M_\infty = 15$)

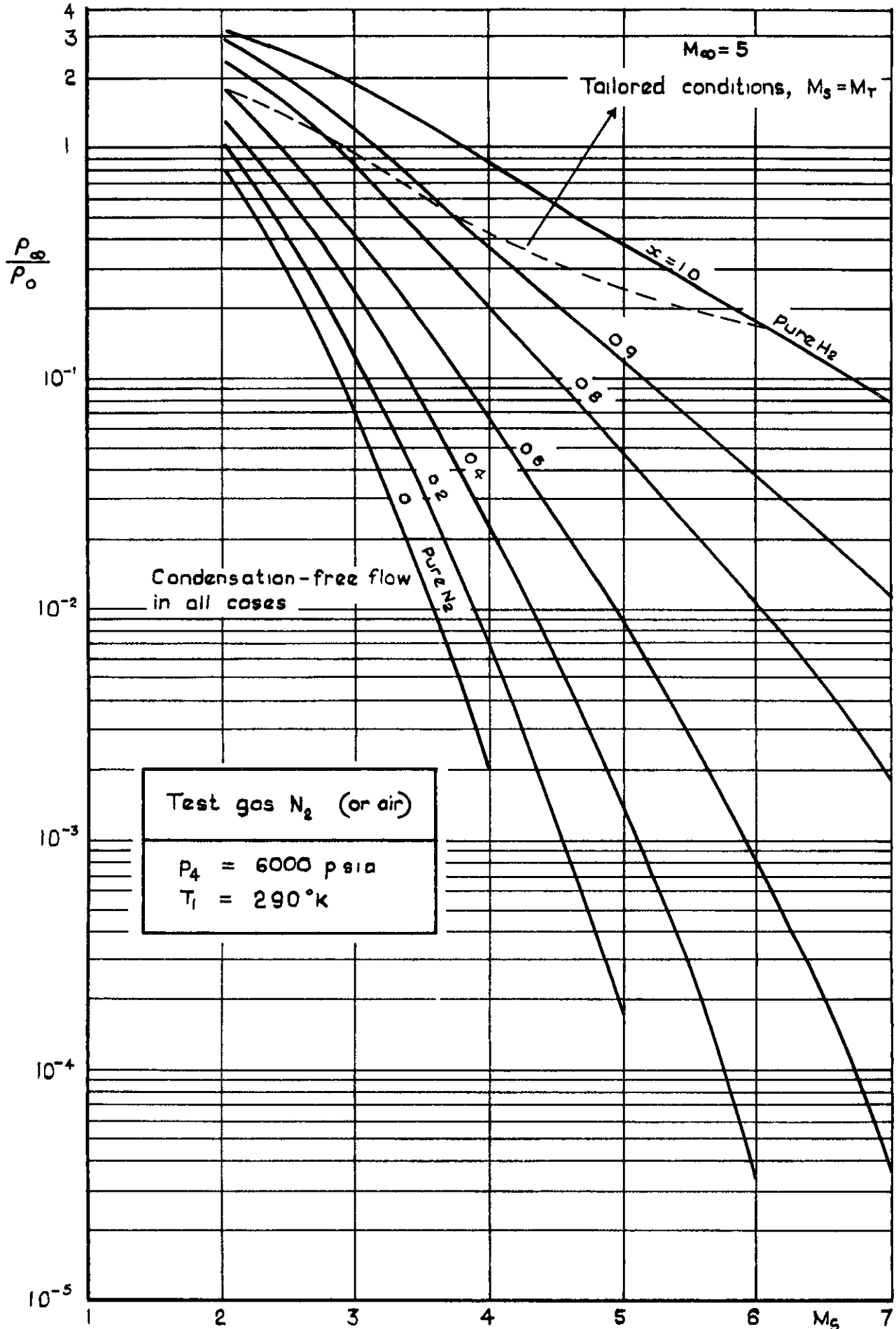

Fig. 17 Ratio of density in the working section, ρ_∞, to atmospheric density, ρ_0, versus incident-shock Mach number, M_S, for various values of the particle concentration parameter, x. ($M_\infty = 5$)

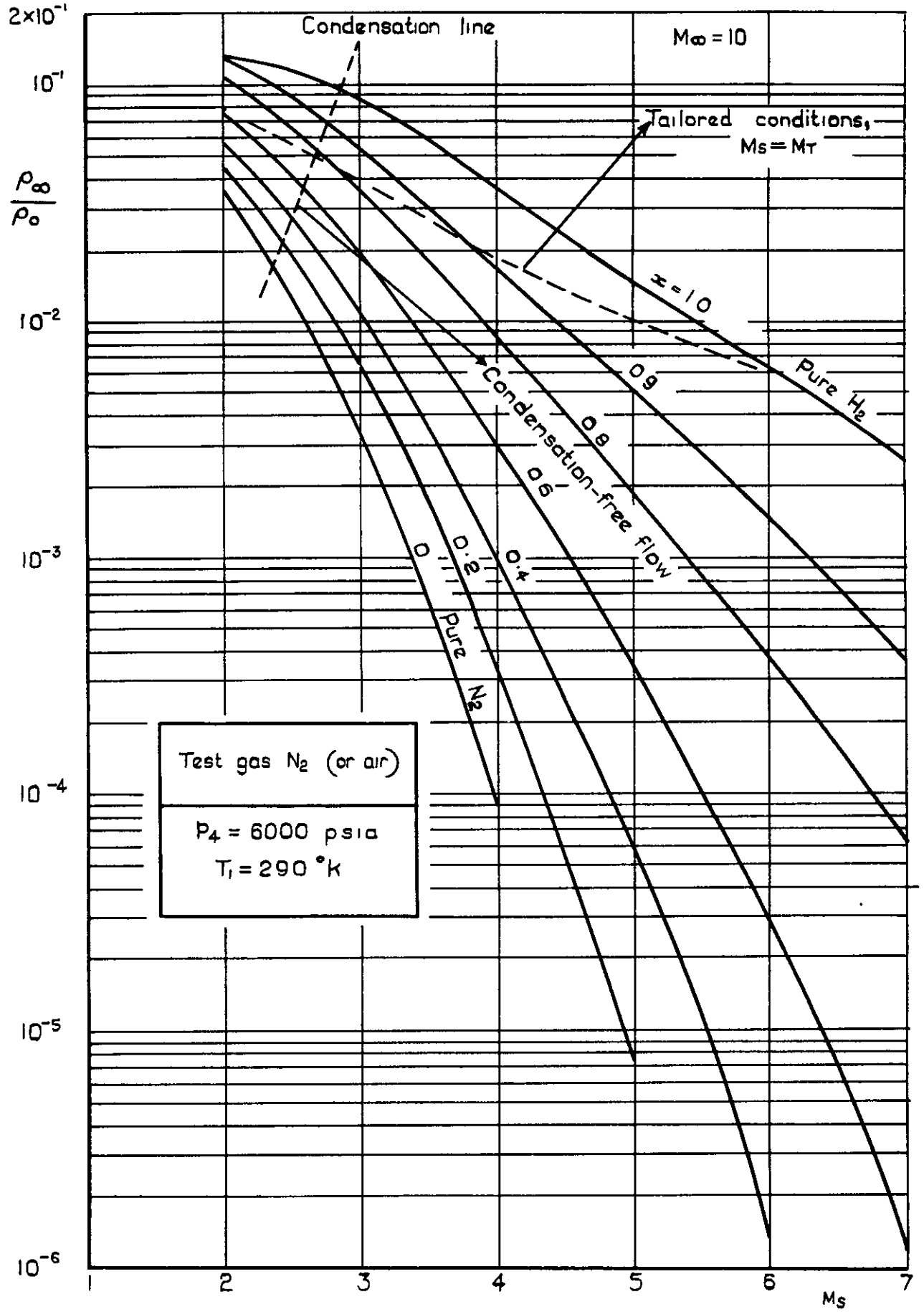

Fig. 18 Ratio of density in the working section, ρ_∞, to atmospheric density, ρ_o, versus incident – shock Mach number, M_S, for various values of the particle concentration parameter, x. ($M_\infty = 10$)

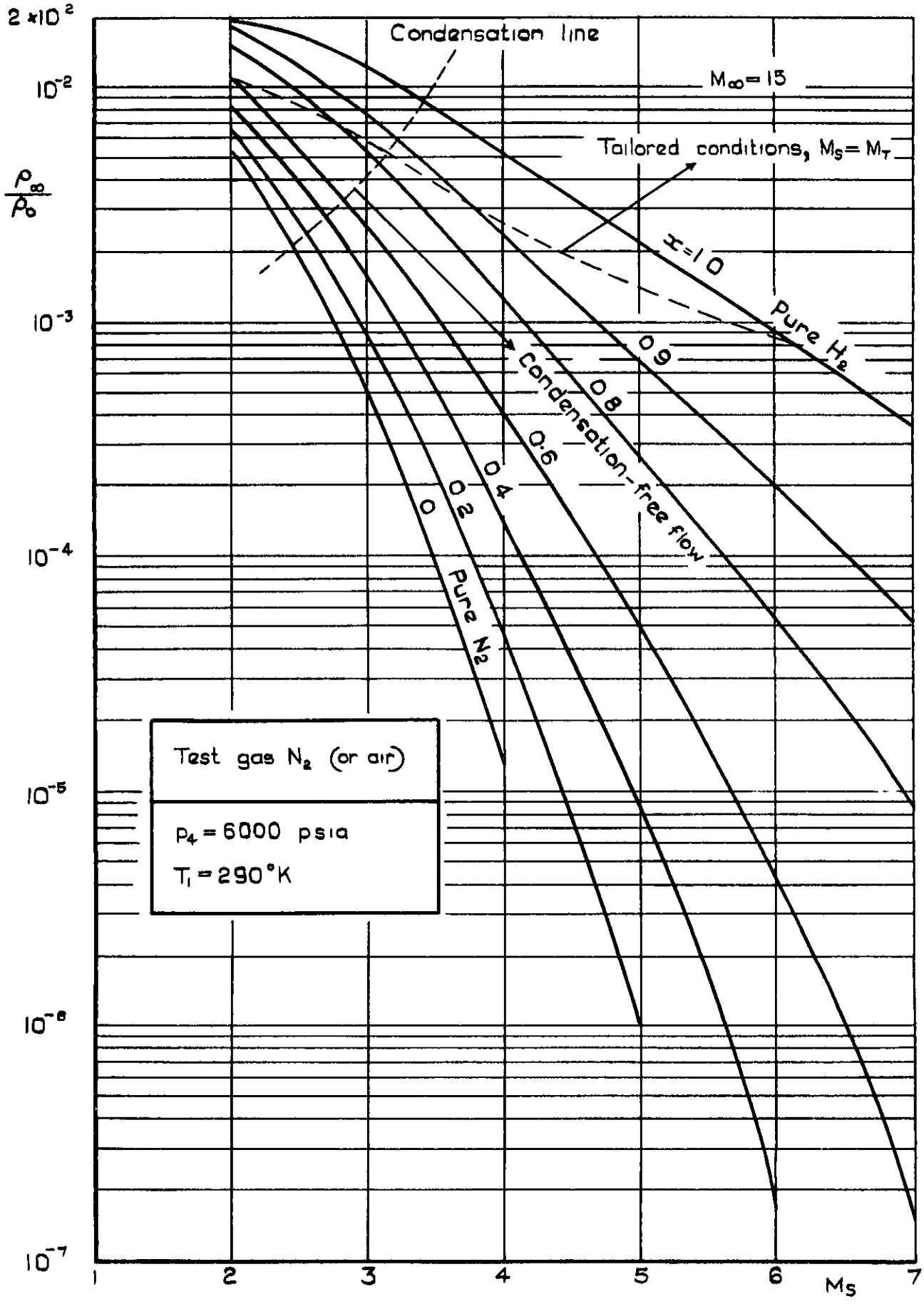

Fig. 19 Ratio of density in the working section, ρ_∞, to atmospheric density, ρ_0, versus incident-shock Mach number, M_S, for various values of the particle concentration parameter, $\varkappa$. $(M_\infty = 15)$

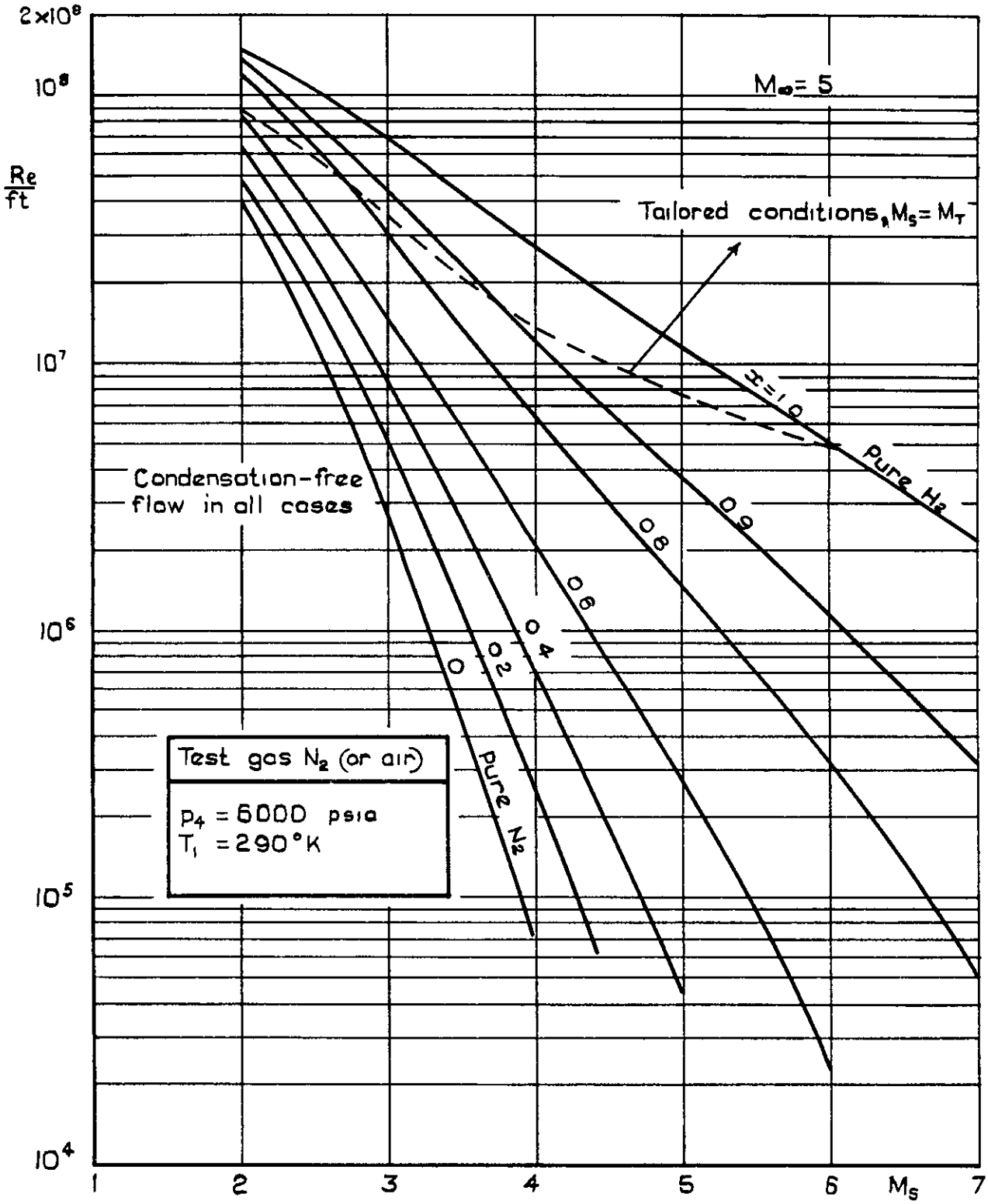

Fig. 20 Reynolds number per foot in the working section versus incident-shock Mach number, M_S, for various values of the particle concentration parameter, x, ($M_\infty = 5$)

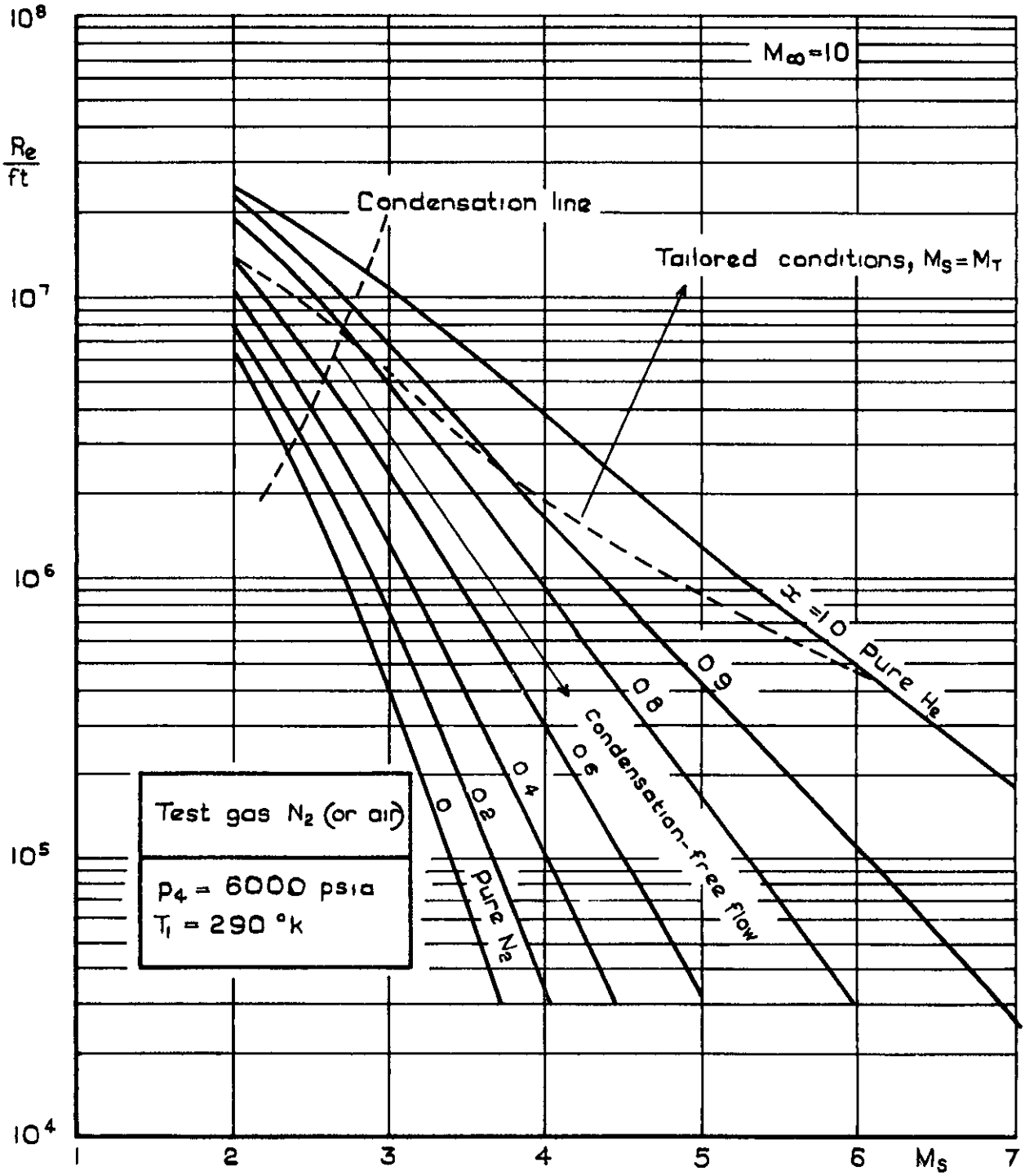

Fig. 21 Reynolds number per foot in the working section versus incident-shock Mach number, M_S, for various values of the particle concentration parameter, χ. ($M_\infty = 10$)

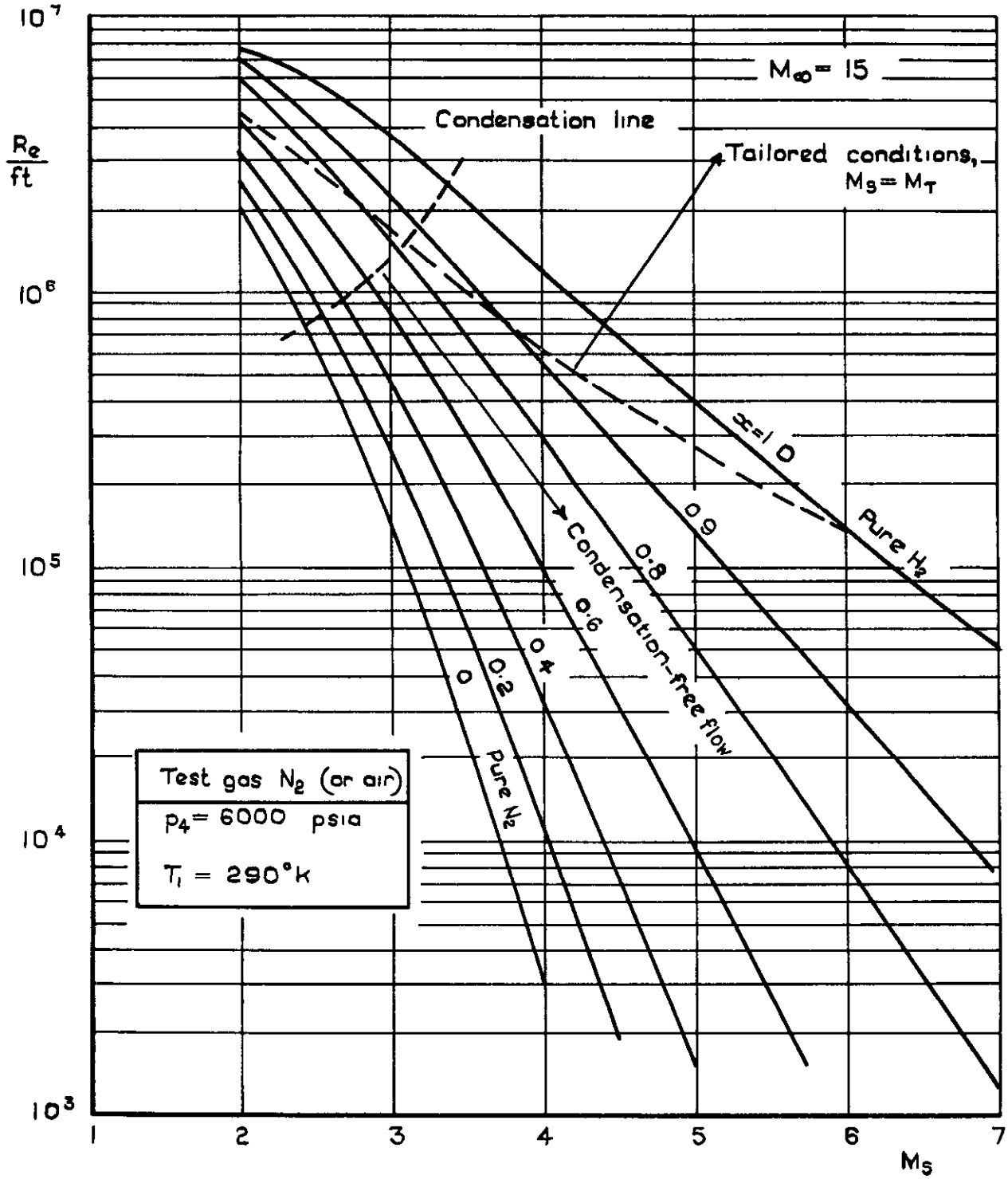

Fig. 22 Reynolds number per foot in the working section versus incident-shock Mach number, M_S, for various values of the particle concentration parameter, α. ($M_\infty = 15$)

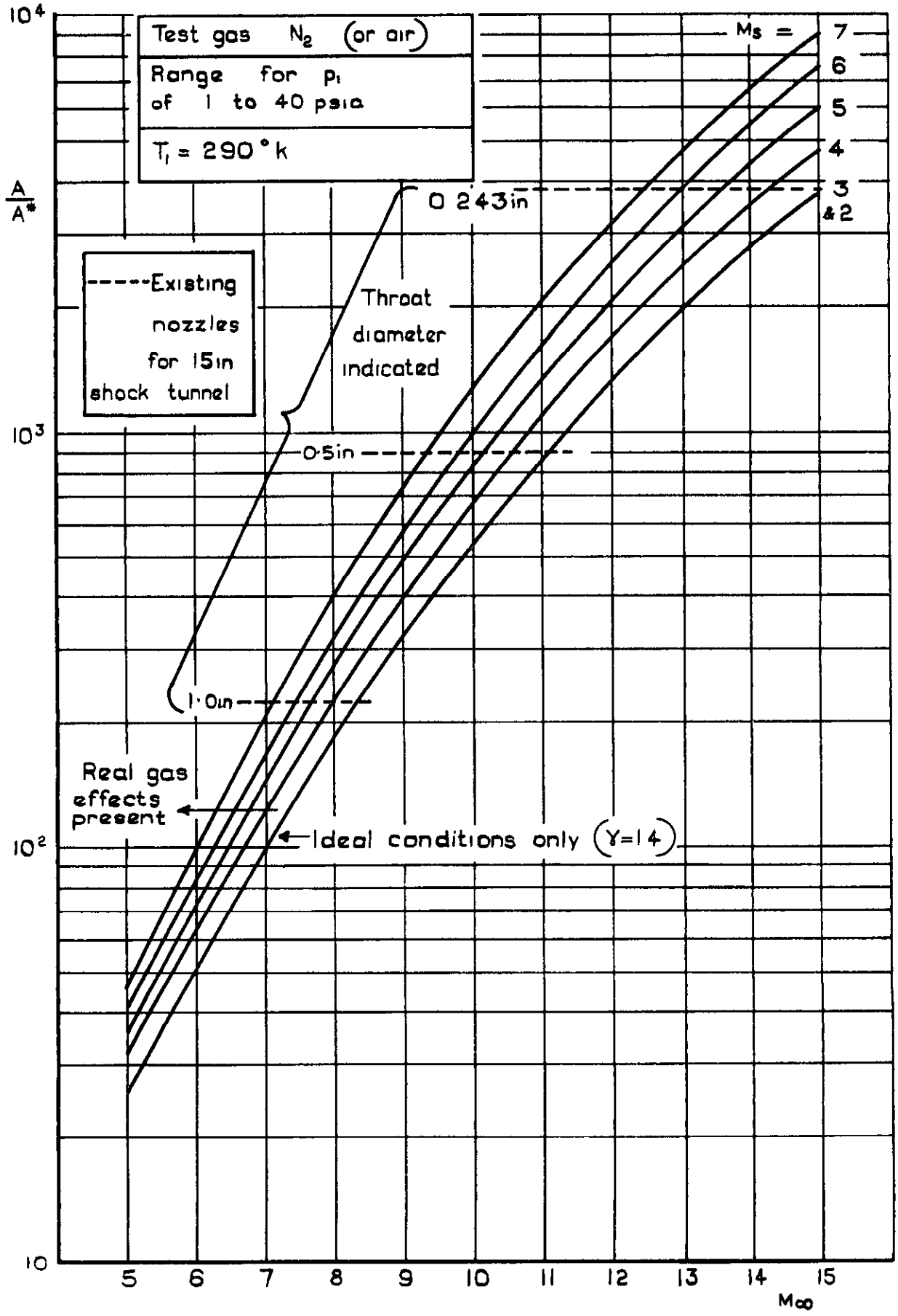

Fig. 23 Ratio of working section cross-sectional area, A, to throat area, A^*, versus the working section Mach number, M_∞, for values of the primary shock Mach number, M_S

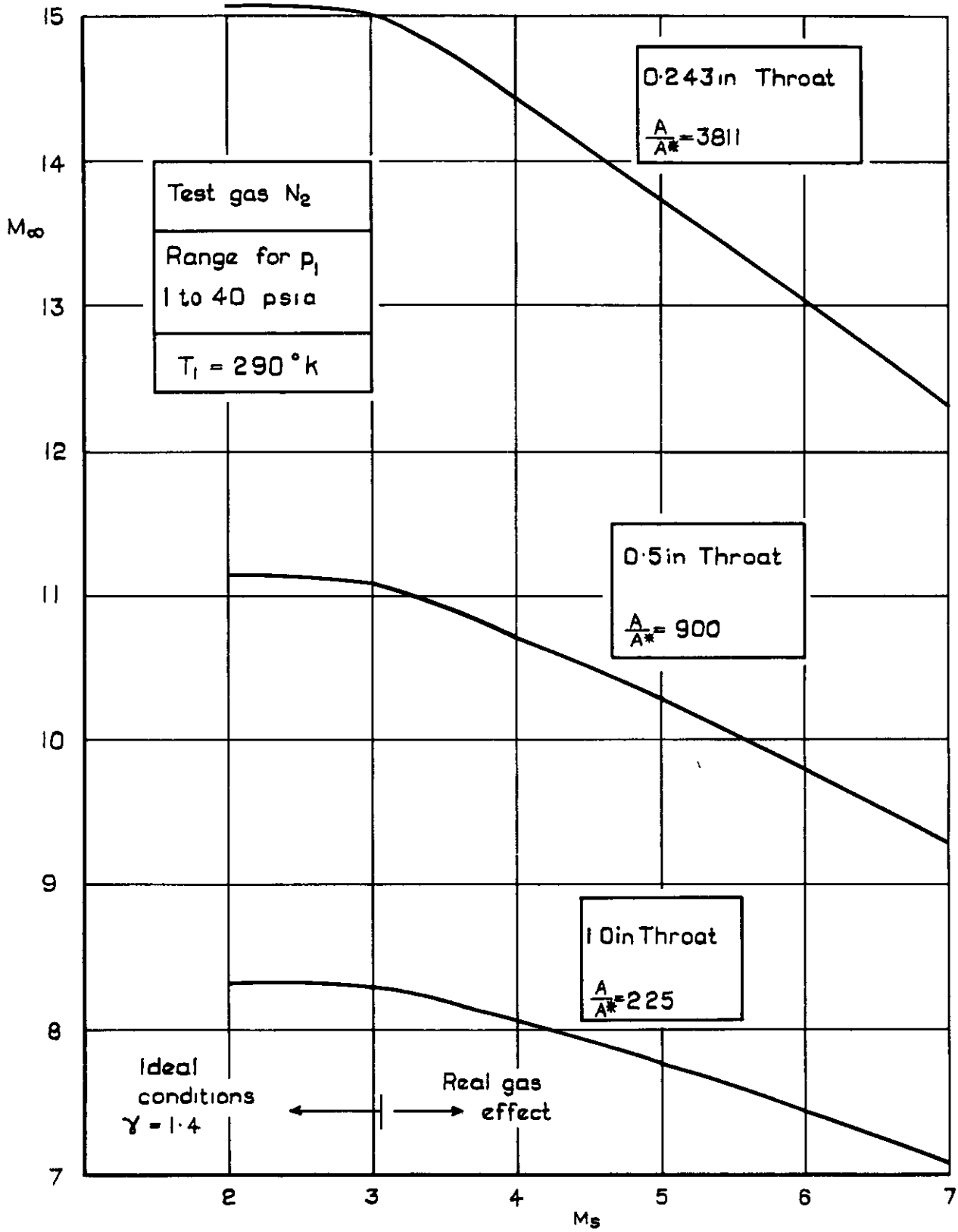

Fig. 24 Variation of Mach number in working section, M_∞, with primary shock Mach number, M_S, for the existing nozzles of the R.A.E. 15in reflected-shock tunnel

Printed in England for Her Majesty's Stationery Office by
The Royal Aircraft Establishment, Farnborough. Dd.146915. K.3.

A.R.C. C.P. No.1057
November 1968

533.6.071.8:
533.6.071.4

Woodley, J.G.

PERFORMANCE ESTIMATES FOR A REFLECTED-SHOCK TUNNEL WITH A MODIFIED DRIVER TO PRODUCE HIGH TEST-SECTION REYNOLDS NUMBERS

Some calculations based on the performance of an ideal shock-tube are presented. These demonstrate the possibility of achieving a high test-section Reynolds number in a reflected-shock tunnel, employing nitrogen or air as the test gas, by the use of a driver gas composed of a mixture of hydrogen and nitrogen.

A.R.C. C.P. No.1057
November 1968

533.6.071.8:
533.6.071.4

Woodley, J.G.

PERFORMANCE ESTIMATES FOR A REFLECTED-SHOCK TUNNEL WITH A MODIFIED DRIVER TO PRODUCE HIGH TEST-SECTION REYNOLDS NUMBERS

Some calculations based on the performance of an ideal shock-tube are presented. These demonstrate the possibility of achieving a high test-section Reynolds number in a reflected-shock tunnel, employing nitrogen or air as the test gas, by the use of a driver gas composed of a mixture of hydrogen and nitrogen.

A.R.C. C.P. No.1057
November 1968

533.6.071.8:
533.6.071.4

Woodley, J.G.

PERFORMANCE ESTIMATES FOR A REFLECTED-SHOCK TUNNEL WITH A MODIFIED DRIVER TO PRODUCE HIGH TEST-SECTION REYNOLDS NUMBERS

Some calculations based on the performance of an ideal shock-tube are presented. These demonstrate the possibility of achieving a high test-section Reynolds number in a reflected-shock tunnel, employing nitrogen or air as the test gas, by the use of a driver gas composed of a mixture of hydrogen and nitrogen.

Published by
HER MAJESTY'S STATIONERY OFFICE

To be purchased from
49 High Holborn, London w.c.1
13A Castle Street, Edinburgh 2
109 St. Mary Street, Cardiff CF1 1JW
Brazennose Street, Manchester 2
50 Fairfax Street, Bristol BS1 3DE
258 Broad Street, Birmingham 1
7 Linenhall Street, Belfast BT2 8AY
or through any bookseller

C.P. No. 1057

SBN 11 470184 9